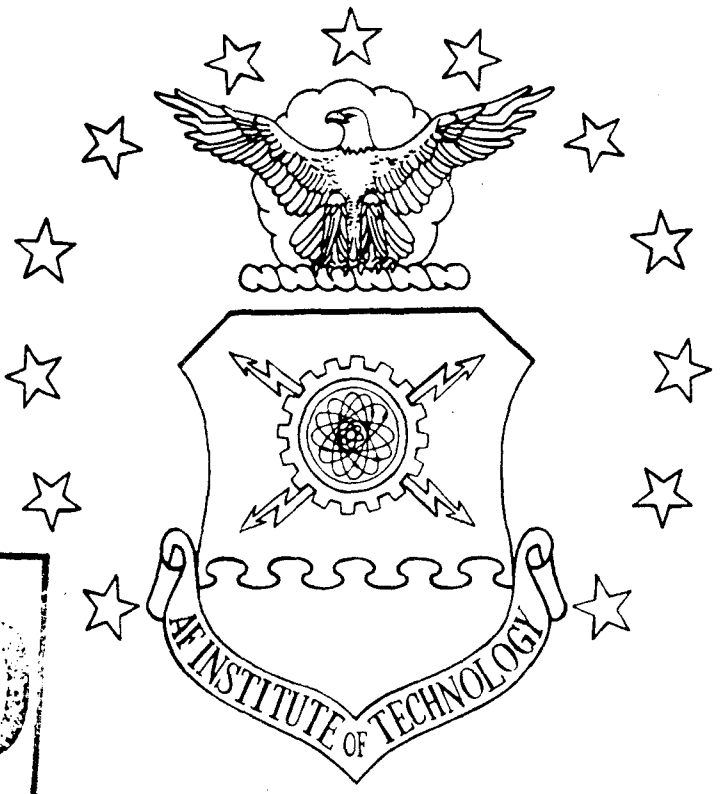

DTIC
SELECTE
JAN 0 4 1994
F

A Numerical Model to Predict the Fate of Jettisoned Aviation Fuel

THESIS

Karl Durant Pfeiffer
Captain, USAF

AFIT/GAE/ENY/94D-01

This document has been approved for public release and sale; its distribution is unlimited.

UNITED STATES AIR FORCE

AIR UNIVERSITY

AIR FORCE INSTITUTE OF TECHNOLOGY

Wright-Patterson Air Force Base, Ohio

19941228 088

AFIT/GCS/ENC/94D-01

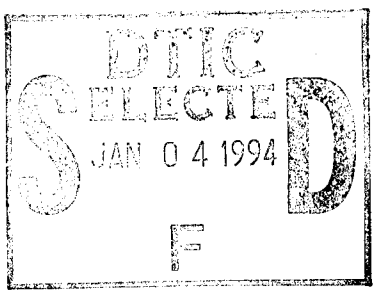

A Numerical Model to Predict the Fate of Jettisoned Aviation Fuel

THESIS
Karl Durant Pfeiffer
Captain, USAF

AFIT/GCS/ENC/94D-01

Accesion For
NTIS CRA&I ☒
DTIC TAB ☐
Unannounced ☐
Justification
By
Distribution /
Availability Codes
Dist | Avail and / or Special
A-1

DTIC QUALITY INSPECTED 2

Approved for public release; distribution unlimited

AFIT/GCS/ENC/94D-01

A Numerical Model to Predict the Fate of Jettisoned Aviation Fuel

THESIS

Presented to the Faculty of the School of Engineering
of the Air Force Institute of Technology
Air University
In Partial Fulfillment of the
Requirements for the Degree of
Master of Science (Computer Science)

Karl Durant Pfeiffer, B.S.
Captain, USAF

December 1994

Approved for public release; distribution unlimited

Acknowledgements

I am deeply indebted to the patience and wisdom of my thesis advisor Dr Dennis Quinn for the many hours he endured my presentations that began with "I have an idea ..." Under his guidance I have grown as a researcher and a scientist.

I am equally indebted to the many hours of conversation and suggestions from Capt Cliff Dungey. His patience and good humor allowed me to keep the problem at hand in perspective.

I wish also to thank Dr Eugene Santos for fielding thorny design and coding questions from a budding computer scientist. His open door and ready response to e-mail helped me reduce my problem domain to a manageable space.

This research could not have been accomplished without the tireless support of the AFIT Technical Library and the computer resources support staff in AFIT/SC. My thanks and appreciation go to these folks for providing an environment where so many technical details become transparent; their efforts gave me the tools to focus on the research problem at hand.

My deepest and humblest thanks I reserve for my wife, Karen, and my son, Karl. They endured every moment of this thesis with unwavering love, unflinching support, and remarkable good humor. Their understanding held our family together through this experience. We are a better family, and I have a better thesis, because of their patience and love.

Karl Durant Pfeiffer

Table of Contents

List of Figures

List of Tables

Abstract

While airborne, military and civilian aircraft must occasionally jettison unburned aviation fuel into the atmosphere. This research investigates the fate of a jettisoned fuel (e.g. JP-4, JP-8, etc.) from initial release to final ground fall by numerically modeling the physical phenomena governing the fate of this fuel: evaporation, advection, and dispersion. Using previous work in evaporation and free fall of fuel droplets as a foundation, this thesis presents an integrated evaporation, advection and dispersion model designed to run under the resources of a typical personal computer. This integrated model is capable of using near real-time meteorological data (i.e. vertical profiles of temperature, pressure and wind) in all model calculations. Physical assumptions in the numerical model are presented, along with sample model calculations supporting these assumptions. Model calculations performed for two jettison scenarios show good agreement with previously published results.

A Numerical Model to Predict the Fate of Jettisoned Aviation Fuel

I. Introduction

1.1 Overview

While airborne, military and civilian aircraft must occasionally jettison unburned aviation fuel into the atmosphere. Clewell analyzed individual fuel jettison reports by Air Force aircrews collected from 1 January 1975 to 30 June 1978 [9, 10]. His detailed investigation provides some insight into typical jettison events. Clewell explained that

> To perform their mission, many aircraft are required to take off with a gross weight much higher than their maximum safe landing weight. If an emergency or change in operational plans requires the aircraft to land prematurely, fuel is jettisoned to reduce weight to a safe level. In some cases the nature of an emergency may lessen the airworthiness of the aircraft. In such instances reducing the weight even below the normal landing weight may be desired to permit a slower landing speed and improve control [9:29].

As early as 1959, Lowell developed a computer model to investigate the fate of jettisoned fuel [22, 21, 23]. His work established that jettisoning unburned fuel at most altitudes presented little or no flammability hazard aloft or at the ground [22, 21, 23]. In the 1970's, the United States Air Force (USAF) began comprehensive research into the fate of jettisoned fuel, culminating in a series of technical reports by Clewell. In addition to investigating the frequency and nature of fuel jettison events within the Air Force [9, 10], Clewell also investigated the evaporation and dispersion of JP-4 with a computer model [8]. Clewell used Lowell's work as a foundation but incorporated more detail in the chemical model of JP-4 and in the simulation

physics [8]. Clewell extended his own work with JP-4 by using the same model code to investigate the less volatile JP-8 [11]. Clewell concluded that current (i.e. 1980) Air Force minimum altitudes for fuel jettisoning (1500 meters for tactical aircraft, 6000 meters for strategic aircraft) resulted in a low threat of ground contamination by JP-4 over typical surface temperatures. Clewell found, however, that similar jettisoning events with JP-8 could cause some ground contamination, especially over colder surface temperatures [11:24,26].

1.2 Problem

As the Air Force moves to less volatile aviation fuels (e.g. JP-8), fuel jettisoning by USAF aircraft will pose a greater risk of ground contamination. The preliminary investigations of Lowell and Clewell support this assertion. Their research provides detailed information about *how much* fuel will contaminate the ground after a particular jettison event. An open question remains: *Where* will this fuel make ground fall?

1.3 Scope

This research builds a general simulation to assess the threat of ground contamination by an aviation fuel following a fuel jettison event. For the purpose of this research, we define a jettison event to begin with the first release of fuel from an aircraft and to end when all liquid fuel has made ground fall or has evaporated. Previous work in fuel droplet evaporation (Clewell [8] and Lowell [22]) is extended to include representative meteorological data in the fuel's descent through the atmosphere. This meteorological data will include a representative wind profile so that droplet position can be modeled in four dimensions (longitude and latitude as well as altitude and time of descent). This extended evaporation and transport model will predict the ground fall and time of impact of the center of mass of the jettisoned fuel. Output from this model is used as input to a dispersion model that

predicts ground-level deposition concentrations (mass per area) at the site of liquid fuel impact.

1.4 Approach

We create a tool for predicting the threat of ground contamination by jettisoned aviation fuel. We assess both the amount of liquid fuel to make ground fall and the location and deposition concentrations of the resulting plume. In this thesis, we

1. Reconstruct and generalize the free fall and evaporation model of Lowell and Clewell. Verify output from this model with published results, using both JP-4 and JP-8.
2. Extend Clewell's model to use actual weather data in droplet descent. Verify output from this model using temperature data that simulates the original standard atmospheric profiles used by Clewell and Lowell.
3. Incorporate wind profile data as part of the meteorological data to predict the horizontal transport of the center of mass of the liquid fuel. Verify this model output using order-of-magnitude estimates from the literature.
4. Develop a dispersion model capable of using the output from our evaporation model to arrive at ground-level isopleths of deposition concentration at a particular horizontal coordinate (or set of coordinates). Verify this model output using the order-of-magnitude estimates from the literature as well as estimates from our previous work.

1.5 Design Considerations

Our model code runs under the resources of a typical personal computer (e.g. i386 or i486 architecture), although it is portable enough to move easily to similar or more advanced architectures (e.g. DEC VAX or RISC workstations). Further,

we acknowledge from the beginning that the code will (hopefully) be examined and improved by follow-on research. We take care, then, to ensure the code is

- Understandable.
- Extendable.
- Portable.

1.6 Summary of Thesis

The thesis is organized as follows:

Chapter II reviews current knowledge in determining the fate of jettisoned aviation fuel.

Chapter III presents our model design and implementation.

Chapter IV presents results from our evaporation, transport and dispersion modeling, with comparisons to and validation against previous research.

Chapter V summarizes our research and conclusions and presents recommendations for further research.

Appendix A presents the detailed fuel component models used in this research, originally formulated by Clewell.

Appendix B presents a user's guide to the evaporation, advection, and dispersion model developed in this research.

Appendix C contains the complete code lising for the **getmet** utility, used to extract model-ready atmospheric data files from World Meteorological Organization (WMO) formatted data files, available over internet.

Appendix D contains the complete code listing for the **makestd** utility, used to create model-ready atmospheric data files based on a surface temperature and the standard atmosphere.

II. Background

2.1 Overview

Given a particular jettison event, we want to answer the question: *Where and to what extent will aviation fuel contaminate the ground?* Our methodology is to numerically simulate the primary physical phenomena that govern the fate of the jettisoned fuel. These processes can be loosely grouped into evaporation, dispersion, and advection. Evaporation and dispersion determine how much and in what concentration liquid fuel will make ground fall. Advection determines where this point of impact will be. Implicit in each of these phenomena is the additional requirement to characterize the atmosphere with temperature, pressure and wind data. Before discussing our model design and implementation, we first present a review of relevant research in characterizing and simulating these processes.

2.2 Lowell, 1959

Lowell simulated the evaporation of aviation fuel by modeling the evaporation characteristics of individual fuel droplets over a range of diameters, then scaling these findings to the original problem by treating the plume of jettisoned material as a continuous distribution of these droplets [22, 23]. Lowell used a ten-component synthetic mixture to numerically represent JP-4 [22] and later JP-1 [23]. Lowell's model was composed of two interdependent modules: a free fall model and an evaporation model. The free fall model calculated the change in the altitude of the droplet using a computed terminal velocity and a fixed time interval. The evaporation model calculated simultaneously (i.e. over the same time interval) the mass evaporated from the droplet. This change in mass and diameter (as well as change in local air temperature because of the change in altitude) were used at the beginning of the next time interval to compute a new terminal velocity and corresponding change in altitude [22:9–13]. Air temperature at altitude was derived assuming a standard atmosphere.

The standard atmosphere is a reference, or mean, profile of temperature and pressure with altitude, maintained by the International Civil Aviation Organization (ICAO) and compiled and extended for the United States by the National Oceanic and Atmospheric Administration (NOAA) [32]. Different atmospheric temperature profiles were simulated by using different sea-level temperatures to calculate the standard atmosphere relations.

In his original work with JP-4, Lowell concluded that the "principal controlling variable" in determining mass-loss was air temperature [22:1]. Lowell assumed initially that droplet temperature was always in equilibrium with air temperature. The implication of this assumption is that the droplet is immediately at air temperature upon jettison and breakup of the liquid fuel and that in evaporating the droplet never loses any heat (i.e. never cools below air temperature). Lowell justified this assumption by noting that this temperature difference amounts to typically less than 9 C° and would only be significant in warmer (around 30°C) air temperatures where evaporation is relatively rapid [22:13]. Lowell later revisited his work with JP-4 in research on the less volatile JP-1 (similar to commercial kerosene) [23]. As expected, Lowell found that JP-1 did not evaporate as readily as JP-4 under the same jettison conditions. He suggested this difference in evaporation rates could be approximated by observing that JP-1 behaved similarly to JP-4 jettisoned at a surface temperature 20 C° colder [23:7].

For his research with JP-1, Lowell had better computing facilities at his disposal and so increased the complexity of his calculations by including an evaporative cooling routine in this revised code. Although not the original thrust of this research, Lowell does include one figure comparing old (no droplet cooling) results to new results; the cooling routine appears to slow down the evaporation rate by about 3% for a 750 micron (diameter) droplet released at 5000 feet [23:38–39]. Since the original basis for neglecting this droplet cooling was that the fuel (JP-4) was relatively volatile, we can assume that on a less volatile fuel (e.g. JP-1) this cooling routine

would significantly effect the overall evaporation rate of the droplet. In his later work with JP-1, Lowell also implemented an aggressive time step. This aggressive time step was an algorithm in the evaporation computation so that the time step increased as the droplet evaporation rate slowed. Lowell's model calculations for droplet terminal velocity and evaporation were piecewise linear approximations to curves; these curves became more linear as the evaporation rate decreased [22:14–15]. The adaptive time step algorithm economized model calculations by using a larger time step to approximate these almost-linear curve segments [23:9–10]. Lowell established thresholds for mass evaporated and distance fallen in any one interval to regulate the growth of the time step and maintain the integrity of the piecewise linear approximation [23:9–10].

In addition to his computer models of free-fall and evaporation, Lowell also investigated the dispersion of jettisoned JP-4 [21]. Lowell treated the plume of jettisoned material as an infinite, instantaneous line source [21:7-9]. Lowell used this analysis of the problem to assess the potential flammability hazard following a jettison event. Using his free-fall and evaporation data, Lowell computed fuel dispersion test cases by hand and concluded that jettisoning by aircraft at ground clearances greater than 500 feet presented no hazard [21:15]. Lowell carefully restricted his conclusions to flammability, however, noting that assessing ground contamination would require further study [21:15].

Lowell's work centered on the evaporation of droplets as discrete elements in a continuous distribution of droplet sizes. To create the initial conditions following a jettison event, Lowell used the work of Merrington and Richardson on the breakup of liquid jets [21]. After studying the characteristics of several liquids dropped from a tower and from low flying aircraft, Merrington and Richardson suggested the empirical relation

$$\bar{d} = 500\frac{\nu^{0.2}}{V_{rel}} \tag{2.1}$$

where V_{rel} is the relative velocity between the liquid and air in centimeters per second (cm/s), ν is the kinematic viscosity of the liquid in cm^2/s and $\bar{d}$ is the mean drop diameter in centimeters, where "mean" indicates the drop size making the greatest contribution to the mass jettisoned [24]. Lowell, probably using a value of $\nu = 0.018$, calculated $\bar{d} = 180$ microns. In scaling up his droplet evaporation results, however, Lowell used a mean droplet size of 250 microns to ensure conservative results [22:10].

2.3 Cross and Picknett, 1972

Merrington and Richardson investigated a variety of liquids, but of these only carbon tetrachloride was volatile [24]. In August 1972, Cross and Picknett conducted a series of field experiments to characterize the initial drop size distribution of jettisoned Avtag (JP-4) and Avtur (JP-8) fuels [13]. An aircraft flying at an altitude of 15 meters with an airspeed of 120 meters per second (m/s) jettisoned flourescent-tagged fuels through a discharge pipe six centimeters in diameter at a rate of 450 kilograms per minute (7.5 kilograms per second). Droplet data were collected on photographic filter papers along the jettison route [13]. For jettisoning through a port parallel to the airstream, Cross and Picknett found a mass median diameter of 270 microns with a maximum diameter of 680 microns. Using a port normal to the airstream, wind shear is assumed to cause a more efficient breakup resulting in smaller drops; Cross and Picknett found that for such a port, the median diameter was 240 ± 10 microns, while the maximum diameter was 400 ± 15 microns [13]. Qualitatively, Cross and Picknett observed that increasing the air speed reduced drop size, while increasing jettison rate increased drop size. The initial drop distribution appeared to be independent of the aviation fuel type [13].

2.4 Wasson, Darlington, and Billingsley, 1973

Cross and Picknett conducted their studies in 1972. Wasson, Darlington, and Billingsley (hereafter referred to as Wasson), working at the Arnold Engineering De-

velopment Center (AEDC), Arnold Air Force Station, Tennessee, gathered seemingly conflicting data on initial droplet distributions in a series of experiments from 22 October 1973 to 12 December 1973 [25]. Wind tunnel experiments were conducted for airstream velocities from 200 to 400 knots, altitudes from 12,000 to 25,000 feet, and jettison rates from 13 to 290 pounds per minute (0.02 to 2.2 kilograms per second); data were collected in a holography recording system [25]. From these experiments, Wasson concluded that jettisoned JP-4 should break up initially into droplets of 19 to 36 microns in diameter, with a maximum observed size of 100 microns.

2.5 Dawbarn, Nutt, and Pender, 1975

Dawbarn, Nutt, and Pender (hereafter referred to as Dawbarn), also at AEDC, suggested in their comprehensive study of JP-4 jettisoning [14] that the nature of the experiments could account for this disparity in results. Cross and Picknett had sampled far away from the jettison port and had used realistic jettison rates; Wasson had, by design, sampled at and near the port and was constrained by the wind tunnel to use atypically low jettison rates, 0.02 kilograms per second to 2.2 kilograms per second as opposed to 7.5 kilograms per second in the Cross and Picknett study. Dawbarn recorded data both near and far away from the jettison port, with the result that droplets in the range of 40 to 100 microns in diameter were found nearest the port; no drops greater than 100 microns diameter were found greater than 15 feet away from the port. Large droplets (diameter $>$ 2000 microns) were only observed at distances greater than 25 feet from the port [14]. Dawbarn suggested that once the droplets were outside the airstream of the port, smaller droplets decelerated preferentially and fell out nearer the point of jettsion, while larger drops continued away from the port [14]. Although Dawbarn found no experimental evidence to suggest that large droplets are created by coalescence of smaller droplets, he did observe that large droplets could grow significantly after jettison by collision with and assimilation of smaller droplets. Dawbarn also suggested a resolution to a discrepancy in

the results from Cross and Picknett. Cross and Picknett could account for only 55% of the mass jettisoned in tabulating their data. They speculated that their sample collectors may have been shielded by tall grasses, and that smaller drops may have evaporated before reaching the collectors [13]. Dawbarn hypothesized that the missing mass could be explained by a substantial number of small droplets (i.e. diameter < 50 microns) that, with correspondingly small terminal velocities, drifted out of range of the collectors [14]. Dawbarn's work in the breakup of the liquid jet only demonstrated the existence of ranges of drop sizes, however, and did not provide data on size distribution to confirm this hypothesis.

2.6 Clewell, 1980

Contemporary with the AEDC studies, Clewell at the Air Force Engineering and Services Center (AFESC), Tyndall AFB, Florida, conducted extensive research into fuel jettisoning by Air Force aircraft. We have already mentioned Clewell's study on the nature and frequency of fuel jettisoning within the Air Force [9, 10]. Clewell also conducted further research into initial droplet distributions to resolve differences between the experimental data of Cross and Picknett and Wasson at AEDC. Clewell's experiments took in-flight samples with an instrumented Piper Navajo aircraft following a KC-135 aerial refueling tanker. The KC-135 jettisoned fuel in simulation of typical jettison events, dumping fuel through its 10.1 centimeter refueling port (boom) at an airspeed of 170 m/s (about 340 knots), at a jettison rate of 56 kilograms per second (kg/s) [8:20]. As part of this effort, Clewell developed an evaporation model based on Lowell's work to assist in interpreting the experimental results. The sampling aircraft normally passed through the plume 90 seconds after the tanker had passed; results from Clewell's model revealed that a typical fuel droplet had lost more than 80% of its original mass and had been reduced to half its original size within this first 90 seconds of jettison [8:23]. Clewell found a mass-median diameter of 270 microns [8:31], in good agreement with the Cross and

Picknett study. Although Cross and Picknett concluded that at a release height of 15 meters no significant evaporation could take place, their results could not account for more than 55% of the jettisoned mass. Clewell used his evaporation model to simulate the Cross and Picknett study and predicted that 40% of the mass would evaporate in this descent of 15 meters, probably explaining most of the unaccounted fuel [8:34].

Clewell's model was based fundamentally on Lowell's work. Clewell improved Lowell's 10-component model of JP-4 with a 33-component representation that permitted modeling the droplet until 99.9% of the mass had evaporated [8:4]. Clewell also initialized the droplet temperature at the equilibrium temperature of the aircraft fuel tanks, typically warmer than the air temperature at altitude [8:86–87]. Clewell observed that the fuel droplet (as simulated) cooled to equilibrium temperature with air in approximately a minute and had approximately the same chemical composition regardless of temperature. Clewell suggested that for a simulation with a lifetime over one minute, the droplet temperature can be assumed to be at or near local air temperature [8:80–84]. Noteworthy in Clewell's model results are that at jettisons above 1500 meters, increased evaporation does not contribute signficantly to reducing the fuel mass reaching the ground [8:57–58]. Colder air temperatures above 1500 meters will significantly slow evaporation, and the droplet composition itself changes over time to predominantly less volatile components [12].

Clewell later used this same model code to investigate the effect of fuel composition on the potential for ground fall following a jettison event [11]. Using a 27-component model of the less volatile JP-8, Clewell found that at surface temperatures below 0°C approximately 20% of the fuel would reach the ground regardless of jettison altitude [11:24]. Using a 30-component model of Number 2 Diesel Fuel (DF #2) to represent future, broadened-specification fuels, Clewell found that even under extremely warm surface temperatures (around 40°C) about 50% of DF #2 made ground fall [8:13]. In summarizing his work with fuel jettisoning in the *AIAA Jour-*

nal of Aircraft, Clewell recommended the Federal Aviation Administration (FAA) guidance to civilian airlines to jettison above 600 meters be amended to the Air Force standards of 1500 meters for small aircraft and 6000 meters for larger aircraft [12]. Civilian airlines use primarily JP-8. While little significant evaporation will take place after 1500 meters of descent under most atmospheric conditions, Clewell noted that the increased time of descent allowed atmospheric processes to further disperse the fuel and reduce point ground contamination [12]. Clewell, however, gives only a cursory treatment of dispersion in his research, using a simple box model to determine the upper limit of ground concentration [8:74].

2.7 Summary

Our review of the literature suggests that of the processes governing the fate of jettisoned fuel, evaporation is the most thoroughly researched and modeled. The experimental research of Cross and Picknett and AEDC validated the early modeling work of Lowell and provided a basis for Clewell's research in droplet evaporation. Clewell's results for JP-4 demonstrated that the Air Force standard jettisoning altitudes were sufficient to prevent significant ground contamination. Clewell's results for JP-8 and DF #2, however, suggest that we can not examine evaporation alone to fully assess the threat of ground contamination. We conclude that our research should address advection and dispersion in detail, atmospheric processes previously given only minimal treatment in the context of this problem. We also seek to move beyond the standard atmosphere assumptions of previous research and better represent the atmosphere in our overall analysis.

III. Model Design and Implementation

3.1 Overview

Lowell noted that determining the fate of jettisoned fuel requires characterizing many elusive physical phenomena, concluding that "... a completely general solution is merely a goal [22:2]." We now present our solution.

We first characterize the initial conditions for a jettison event, identifying our assumptions in the overall simulation. We next describe the structure of the simulation, describing how we model the critical processes: environment, evaporation, advection, and dispersion. We then present each of these component models, outlining critical assumptions and physical principles.

3.2 Initial Conditions

3.2.1 Plume Composition. We assume the jettisoned plume is a monodisperse system; that is, we assume the plume consists of a continuous distribution of fuel droplets, all of the same diameter. Clewell found good agreement between evaporation model predictions for a single droplet at mass median diameter for a KC-135 (270 microns) and other distributions of droplets. His conclusion was that "the central tendency ... of the droplet sizes is relatively unimportant for determining the composite evaporation and free fall of the distribution [8:60]." We conclude, then, that this assumption is reasonable and representative.

3.2.2 Plume Geometry. We have described the temporal character of a jettison event as beginning with the first fuel release. We assume that the initial plume of jettisoned fuel is created by an aircraft flying at fixed speed, altitude, and heading, using a constant release rate. A review of Clewell's record of Air Force jettison events [10] suggests that these assumptions are reasonable; typically, we will not have better information with which to formulate initial conditions. Of

these assumptions, perhaps the least representative of the physical reality is that the initial plume is a single straight line. Clewell reported that a typical dumping pattern, called a racetrack, involves a two minute downwind leg, a two minute turn, a two minute upwind leg, and another two minute turn [9:34]. We argue that we could simulate a racetrack as a series of four or more straight segments, each segment used as an initial condition to a complete model run.

3.2.3 Plume Tilt. We assume not only that our plume is straight, but also that the plume begins at a single altitude. This is equivalent to assuming that the plume is jettisoned instanteously. This simplification causes error in calculating plume length both at the initial release and at ground fall.

We first consider the initial error ϵ_0. The assumed initial plume length is

$$L_0 = V_a \Delta t \tag{3.1}$$

where V_a is the aircraft airspeed and Δt is the total duration of the release. We define the trailing edge of the plume to be that end of the plume first released by the aircraft; similarly, we define the leading edge of the plume to be the last of the material released from the aircraft. This formulation (Equation 3.1) is not the actual plume length because the trailing edge of the plume has moved both vertically and horizontally before the release of the leading edge. We assume the releasing aircraft is flying compass heading ϕ, and that the mean wind U is coming from α. We further assume the terminal velocity V_t of the plume material, identical to the terminal velocity of the droplets, is approximately constant. Figure 3.1 shows this initial geometry. The actual plume length L can be written as

$$L = \sqrt{(x_l - x_t)^2 + (y_l - y_t)^2 + (z_l - z_t)^2} \tag{3.2}$$

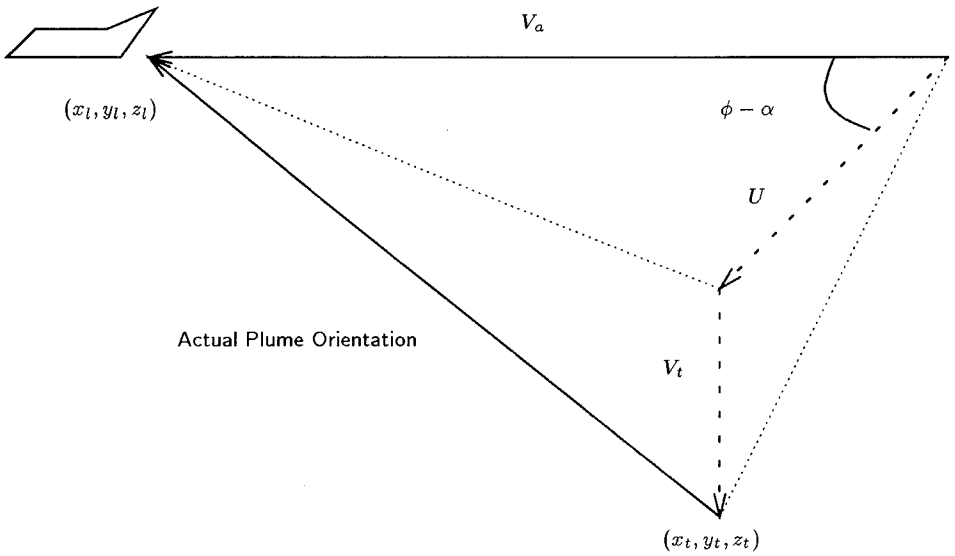

Figure 3.1 Plume tilt geometry after initial release

where

$$x_l - x_t = V_a \Delta t - U \cos(\phi - \alpha)\Delta t$$
$$y_l - y_t = U \sin(\phi - \alpha)\Delta t$$
$$z_l - z_t = V_t \Delta t$$

We define our error ϵ_0 to be

$$\epsilon_0 = 1 - \frac{L_0}{L} \tag{3.3}$$

Substituting Equation 3.1 and Equation 3.2 into this relation simplifies to

$$\epsilon_0 = 1 - \left[\left(\frac{V_t}{V_a}\right)^2 + \left(\frac{U \sin(\phi - \alpha)}{V_a}\right)^2 + \left(1 - \frac{U \cos(\phi - \alpha)}{V_a}\right)^2 \right]^{-1/2} \tag{3.4}$$

From Clewell's model output, we estimate V_t for JP-4 droplets at about one meter per second (m/s) [8:108–118]. We use order of magnitude estimates $U = 10$

m/s and $V_a = 10^2$ m/s to estimate ϵ_0.

Upwind release	$\phi - \alpha = 0°$	$\epsilon_0 = -0.01$
Downwind release	$\phi - \alpha = 180°$	$\epsilon_0 = 0.01$
Crosswind release	$\phi - \alpha = 90°, 270°$	$\epsilon_0 = 0.005$

We choose to neglect this error.

Another possibly significant effect of plume tilt occurs at ground fall. As the tilted plume of liquid fuel intersects the ground, the trailing edge be removed from the plume by deposition (ground fall). The leading edge of the plume will be stretched by near-surface winds over the time interval required for the leading edge of the plume to make ground fall. The plume terminal velocity, assumed identical to droplet terminal velocity, will decrease as the material evaporates on descent. Clewell reported model results that showed droplet terminal velocities decreasing by one to two orders of magnitude in a 1500 meter descent [8:108–118]. If we assume negligible dispersion of the plume along its length, plume length is approximately L_0 at ground fall. Assuming an approximately constant ground fall terminal velocity V_{tg} and mean surface wind U_{sfc}, stretched plume length L_s is

$$L_s = L_0 + U_{sfc}\left(\frac{V_t}{V_{tg}}\Delta t\right) \tag{3.5}$$

Defining ϵ_s similarly to the previous analysis, we have

$$\epsilon_s = 1 - \frac{L_0}{L_s} = 1 - \frac{1}{1 + (V_t U_{sfc})/(V_{tg} V_a)} \tag{3.6}$$

This is in accordance with our intuition that the error increases with increasing wind speed and with a larger ratio of initial to final droplet terminal speed. This analysis, however, neglects the non-linear deceleration of the droplets in free fall, with the result that this ϵ_s is actually an upper bound. The leading edge droplets are larger and will necessarily have higher terminal velocities than trailing edge droplets that

have evaporated over the duration of the release. To some degree the larger leading edge droplets close the distance and reduce the tilt of the plume in the first few minutes of free fall. The initial trailing edge droplets, assumed to have fallen at a constant terminal velocity, actually decelerate quite rapidly (approximately 50% in 10 minutes for JP-4 [8:108–118]). The original descent $V_t \Delta t$ assumed for the trailing edge plume is therefore too large. Because these non-linear decelerations make a less-tractable analysis, in Chapter IV we present model results that confirm that this plume stretch is negligible in the overall solution.

3.2.4 Wake Effects. Immediately upon jettison the plume of fuel is under the influence of the aircraft wake. We do not attempt to model any of the physical forces in the wake. Rather, we consider only the net effect in spreading the initial plume; that is, we assume a particular initial width of plume associated with a particular aircraft or jettison configuration. Clewell neglected wake effects in the free fall and evaporation model, noting that this underestimates initial droplet terminal velocities; that is, the wake tends to push the plume down [8:38–39]. From experimental results, Clewell concluded that this underestimate resulted in an error of about 100 meters in altitude in the overall descent [8:43]. We similarly neglect wake effects in our evaporation and advection model.

3.3 Model Framework

We have described the jettisoned fuel both as a droplet and as a plume. To determine the fate of this jettisoned fuel, we model the effects of environment, evaporation, advection, and dispersion on both plume and droplet.

The environment model is a passive component, created as a source of meteorological data for the active components. In our formulation of the problem, the environment model has no time-like character and is assumed constant over the time scale of the model, Θ.

The active, or temporal, components can be further separated into two models based on the reference frame of the computation:

1. An evaporation and advection model using a reference frame moving with the droplet.
2. A dispersion model using a reference frame moving with the plume of jettisoned fuel.

The evaporation model follows a droplet with vertical and time coordinates. Advection is modeled by assigning the droplet two additional coordinates in a horizontal plane tangent to the surface of the earth. The droplet is treated as an object embedded in the mean wind; horizontal distance traveled is calculated using the wind speed and evaporation time interval.

Dispersion is not as easily computed in the reference frame of the droplet. We choose instead to model dispersion in a reference frame on the plume of jettisoned fuel.

3.4 Environment Model

3.4.1 Model Description. We treat the environment as a table of meteorological attributes ordered by altitude. These meteorological attributes are

- Pressure
- Temperature
- Density
- Viscosity
- Wind speed and direction

Upon receiving a query for data at altitude z, the model searches the table for observations z_{low} and z_{high} such that $z_{low} \leq z \leq z_{high}$. If z is identical to an observation in

the table, that observation is used to return the queried attribute; else the attribute at z is interpolated from data at z_{low} and z_{high}.

3.4.2 Model Initialization. Ideally, the model is initialized with radiosonde data, commonly referred to as upper air data. Several hundred stations worldwide collect upper air data daily at 0000 and 1200 UTC (Universal Time Code, also known as Greenwich Mean Time or GMT) [16:17]. Using ballon-borne radiosonde instruments, these sites report vertical profiles of temperature, humidity, pressure and wind velocity approximately one hour after collection [16:17]. These reports, along with other current meteorological data, are commonly available over public communication networks; Ahlquist [1] provides an extensive review of meteorological data available over the Internet. Appendix C provides a complete description and listing of the **getmet** utility produced in conjunction with this research. This utility creates model-ready atmospheric data files from the raw, teletype upper air data available on the Internet.

Because previous work used a standard atmosphere uniformly warmed or cooled based on surface temperature, we also produced a utility to create model-ready atmospheric data files based on the standard atmosphere and a supplied surface temperature. Appendix D provides a complete description and listing of this **makestd** utility.

3.4.3 Model Physics. Pressure, temperature, and wind are treated as observations in the table. Density and viscosity are calculated on demand.

To interpolate a temperature T at altitude z between observations at z_{low} and z_{high}, we first compute the local lapse rate Γ using:

$$\Gamma = -\left(\frac{T_{high} - T_{low}}{z_{high} - z_{low}}\right) \tag{3.7}$$

T is interpolated with the simple linear rule:

$$T = T_{low} - \Gamma(z - z_{low}) \tag{3.8}$$

Pressure P at z is interpolated using a form of the scale height equation for a hydrostatically balanced atmosphere [17:83].

$$P = P_{low}\left(\frac{T}{T_{low}}\right)^{gM_a/(\Gamma R_0)} \tag{3.9}$$

where

g = acceleration due to gravity = 9.81 m/s^2

M_a = molecular weight of air = 28.96 kg/kmol

R_0 = universal gas constant = 8314 (N $\cdot$ m)/ (K $\cdot$ kmol)

We note that this relation may not recover P_{high} if the hydrostatic assumption is poor; however, we always satisfy $P_{low} \geq P \geq P_{high}$. If the layer is isothermal (i.e. $\Gamma = 0$), P is calculated using a simple linear interpolation between P_{low} and P_{high}.

Wind speed and direction are decomposed into two components: an east-west zonal component and a north-south meridional component. Component wind speed at altitude is interpolated using a simple linear relation similar to Equation 3.8.

Density ρ is calculated assuming air is an ideal gas:

$$\rho = \frac{PM_a}{R_0 T} \tag{3.10}$$

Kinematic viscosity μ is calculated using a relation published in the *U.S. Standard Atmosphere* [32:7]:

$$\mu = \frac{1.458 \cdot 10^{-6} T}{110.4 + T} \tag{3.11}$$

where T, the air temperature at altitude, is assumed to be in Kelvin. The units of μ for this relation are kg$\cdot$m^{-1}s^{-1}.

3.5 Evaporation and Advection Model

3.5.1 Model Description. The evaporation and advection model follows the droplet in time, space, physical dimension and chemical composition. Because we have defined a jettison to last from release to ground fall or evaporation, this model component also determines Θ, the time scale of the simulation. Figure 3.2 depicts an overview of model execution.

We approach the advection of the plume of jettisoned fuel by examining the advection of individual droplets. We assume that a droplet begins with the velocity of the jettisoning aircraft and decelerates into the mean wind flow. This assumption may be very poor for an individual droplet in the plume; turbulent eddies about the mean wind flow will drive a single particle in a random walk about the center of the plume. This is the basis of Lagrangian dispersion modeling (see, for example, Zannetti [34] Chapter 8). We treat dispersion separately, however, and so we accept that our advection model is in fact following the ensemble averaged position of this particle, which should correspond to the center of mass of the plume [27:532–534].

We employ an aggressive time step scheme, similar to previous work [23, 8]; however, we present the details of our application of this adaptive method for the sake of clarity. Each iteration of the model begins with an estimated time step Δt. In calculating the changes in altitude Δz, latitude Δy and longitude Δx, the model algorithm alters this Δt if calculations exceed threshold distances (nominally 100 meters). These constraints on the growth of the time step are necessary to maintain the integrity of our piecewise linear approximations to the nonlinear changes in droplet mass and terminal velocity. The algorithms controlling mass and temperature calculations can also alter Δt, if necessary, to bring these heat and mass losses to within threshold. At the end of the cycle, Δt is doubled and submitted as the first guess for the next iteration. Typical model results reported by Clewell show a time step that increases to the order of tens of minutes near the end of model execution [8:108–118]. This model accounts for both droplet descent and horizontal

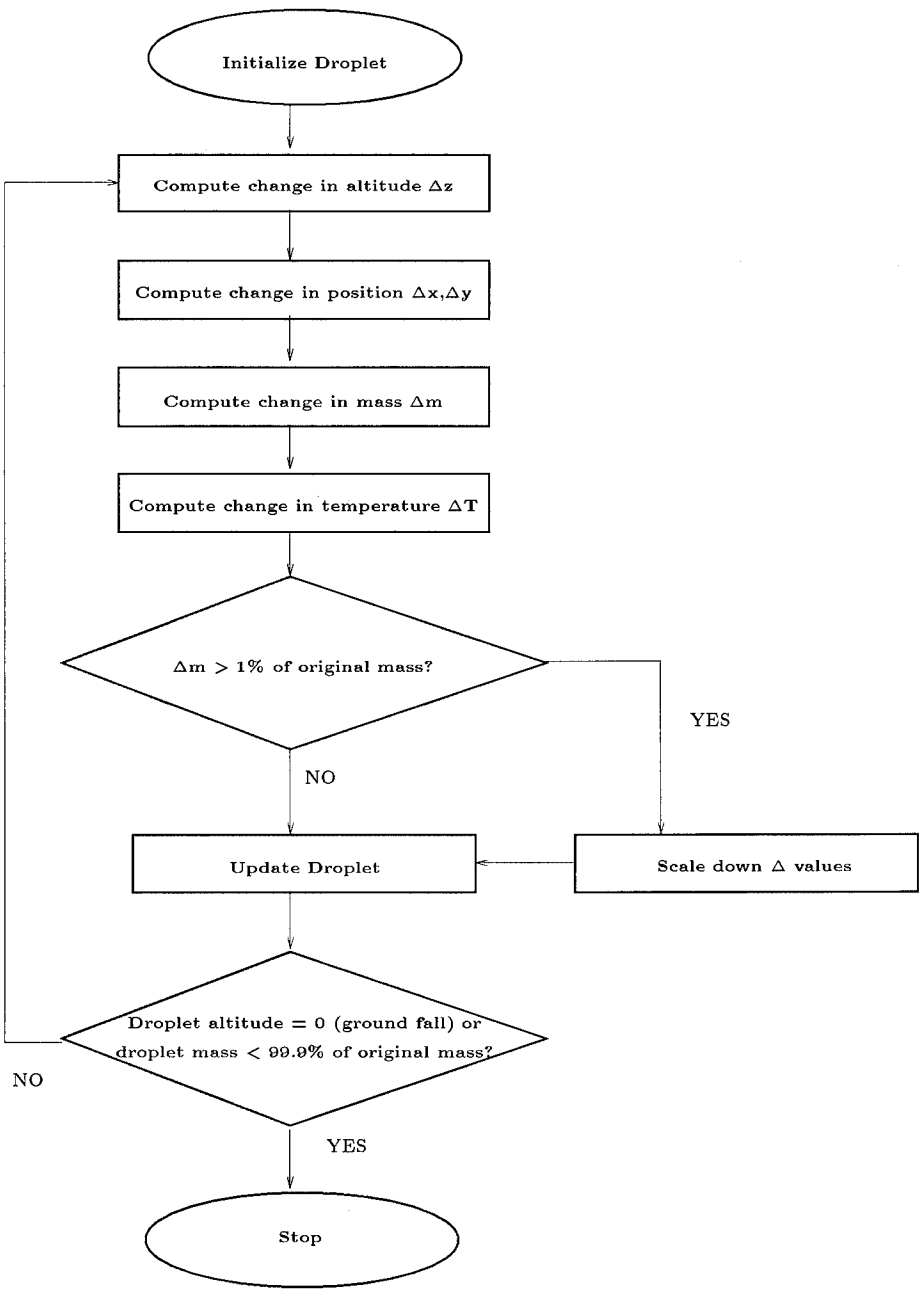

Figure 3.2 The Evaporation Model

translation; wind speed is typically on the order of 10 m/s [19:120–121] while the droplet terminal velocity is initially on the order of 1 m/s [8:108]. Higher wind speeds increase the horizontal displacement of the droplet and induce the model algorithm to reduce Δt and slow model execution noticeably.

We extend previous work in free fall and evaporation by incorporating representative meteorology into droplet descent. Both Lowell and Clewell reported their results in terms of surface temperatures; colder surface temperatures resulted in less evaporation and more ground contamination, warmer surface temperatures resulted in more evaporation and less ground contamination. Using only a standard atmosphere uniformly warmed or cooled to the surface, this approach is insensitive to temperature inversions and other temperature anamolies along the droplet's path of descent. Through the atmosphere, air temperature normally decreases with height; temperature inversions, commonly referred to as inversions, are areas where air temperature increases with height (for a brief discussion of inversions, see Wark and Warner [33:80-81]). In the reference frame on the droplet, passing through an inversion slows down the evaporation rate as the droplet cools on descent. Evaporation calculations over an inversion layer will necessarily yield a different prediction from calculations performed using a standard atmosphere. We present results in Chapter IV that support this assertion.

3.5.2 Model Initialization. Model calculations assume the droplet has an initial chemical composition (e.g. Clewell's 33-component JP-4), an initial altitude equal to the release height of the aircraft, and an initial temperature corresponding to the stagnation, or equilibrium, temperature of the droplet with respect to the aircraft fuel tank. This stagnation temperature T_s is calculated with (see, for example, Holman [18:173–174]):

$$T_s = T_a \left(1 + \frac{(\gamma - 1)V^2}{2{C_s}^2} \right) \tag{3.12}$$

where

$$\begin{aligned} T_a &= \text{air temperature in Kelvin} \\ V &= \text{aircraft airspeed} \\ C_s &= \text{local speed of sound} \\ \gamma &= \frac{C_p}{C_v} = 1.399721 \end{aligned}$$

where C_p and C_v are the specific heat of air at constant pressure and constant volume. Taking $(\gamma - 1)/2 \approx 1/5$, we have

$$T_s = T_a \left(1 + \frac{V^2}{5{C_s}^2}\right) \tag{3.13}$$

which is consistent with Clewell [8:87]. The local speed of sound is calculated with [18:173–174]

$$C_s = \left(\frac{1.4 R_0 T_a}{M_a}\right)^{1/2} = 20.047\sqrt{T_a} \tag{3.14}$$

where R_0 and M_a are the same physical constants defined in the environmental model. This speed of sound calculation is also consistent with Clewell [8:87].

The droplet position is assumed to be the midpoint of the jettisoned plume, calculated based on the reported latitude, longitude, airspeed and heading of the aircraft at the start of the fuel jettison.

3.5.3 Model Physics.

3.5.3.1 Free fall and Evaporation. We use much of Clewell's work in the free fall and evaporation calculations. Clewell, in turn, based much of his model on the work of Lowell. We briefly review the physical assumptions in these calculations.

1. *A droplet is instantaneously at its terminal velocity.* We argue, as did Lowell [22:3], that we can neglect these small accelerations since the terminal velocity

of the droplet is a slowly-varying property of the droplet over most of the time scale of the simulation.

2. *Molecular effects are not significant.* We assume that evaporated molecules do not contribute to the wake of the droplet, nor do they effect the evaporation of neighboring droplets. Once mass has evaporated from the droplet, we no longer consider it part of our model. Lowell noted that this assumption overestimates the evaporation in a plume of material, but hypothesized that vertical dispersion of the droplets because of differing terminal velocities would make this a small effect in the overall solution [22:3]. Dawbarn found that evaporated material in the wake had negligible effect on the terminal velocity of JP-4 droplets [14:35].

3. *Each droplet falls independently.* We ignore the entrainment of smaller drops by larger, and faster, drops. Lowell noted that this assumption would result in terminal velocities that were initially too low [22:3]. We also ignore growth and decay by collision, which is a reasonable assumption given an early vertical dispersion of droplets.

4. *The evaporative behavior of a fuel droplet can be simulated by a mixture of known components.* This is equivalent to assuming that internal mixing in the droplet is sufficient to ensure a uniform distribution of components. Dawbarn studied the evaporation characteristics of JP-4 and concluded that most of the volatile species evaporate early in the descent and so this assumption of internal mixing is justified [14:48].

We compute mass loss following Lowell [22:13] and Clewell [8:88], using a stepwise approximation to the equation:

$$\frac{1}{\pi D^2}\frac{dm_i}{dt} = h_{m,i} p_i \epsilon_i \tag{3.15}$$

where

m_i = mass of the i'th component of the droplet

D = droplet diameter

$h_{m,i}$ = mass transfer coefficient of the i'th component

p_i = vapor pressure of the i'th component

ϵ_i = mole fraction of the i'th component

This approximation becomes

$$\Delta m_i = \pi D^2 h_{m,i} p_i \epsilon_i \Delta t \tag{3.16}$$

where we assume that Δt is sufficiently small so that D, h, p and ϵ are approximately constant. This approach is similar to the treatment of single-component evaporation described in Bird [5:648–649], but extended to multicomponent evaporation assuming Raoult's Law. Raoult's Law states that the i'th component in a multicomponent mixture at reference temperature T exerts a vapor pressure

$$p_i = p_0 \epsilon_i \tag{3.17}$$

where p_0 is the vapor pressure of the pure chemical species at T and ϵ_i is the mole fraction of the species in the mixture [3:222–223].

After calculating the new droplet mass m from the previous droplet mass m_0 (i.e. $m = m_0 - \Delta m$), we calculate a new density, component by component, following Clewell [8:87]. We calculate the new droplet volume by summing over the n components of the fuel mixture:

$$V = \Sigma_{i=1}^{n} V_i = \Sigma_{i=1}^{n} \frac{m_i}{\rho_i} \tag{3.18}$$

where m_i is the new mass of the i'th component and ρ_i is the new density of the i'th component. We assume the droplet is always a perfect sphere, so that

$$V = \frac{4}{3}\pi r^3 \tag{3.19}$$

Substituting Equation 3.19 into Equation 3.18 and solving for r yields

$$r = \left(\frac{3}{4\pi} \Sigma_{i=1}^{n} \frac{m_i}{\rho_i} \right)^{1/3} \tag{3.20}$$

Using the change in mass Δm, we compute a heat balance and the corresponding change in droplet temperature ΔT. In addition to heat lost by mass transfer, Clewell considered heating of the droplet by solar insolation [8:92,94], and we follow this in our calculations. The stagnation temperature (Equation 3.12) used to initialize the droplet typically will be higher then environmental air temperature. We bring the droplet into thermodynamic balance by requiring that the mass loss in any interval be no more than what our step-wise calculation of heat-loss can bring into a steady-state temperature with the local air temperature [8:95]. Clewell observed that for simulations over one minute, the droplet can be assumed to be at air temperature with negligible effect on the solution [8:82,84]; however, we keep the theromdynamic balance calculations as part of our model.

3.5.3.2 Advection. We treat horizontal droplet motion using two-dimensional rectangular coordinates aligned meridionally (north-south) and zonally (east-west). We assume the droplet begins with the speed of the jettisoning aircraft and decelerates into the mean wind. To model the droplet in two dimensions, we perform a one-dimensional analysis then generalize the results to two dimensions. In one dimension, Newton's Second Law is:

$$m\frac{dV}{dt} = F \tag{3.21}$$

where we assume the net force F on the droplet is identical to the drag force. Drag force on an immersed body can be calculated with [28:360]:

$$\text{Drag} = C_d A \frac{\rho V_{rel}^2}{2} \tag{3.22}$$

where

C_d = drag coefficient

A = projected surface area in the flow

ρ = density of the fluid, in this case air density

V_{rel} = velocity of the free-stream fluid flow

Mass m can be replaced with droplet density ρ_d and droplet volume, assuming a spherical droplet of radius r

$$m = \frac{4}{3}\pi r^3 \rho_d \tag{3.23}$$

Substituting expressions for drag force (Equation 3.22) and mass (Equation 3.23) into Equation 3.21 yields the differential equation:

$$\frac{dV}{dt} = \frac{3\rho}{8\rho_d r} C_d (U - V)^2 \tag{3.24}$$

where U is the wind speed and $V_{rel} = U - V$. If we assume the droplet has initial airspeed V_0 at time $t = 0$, we have:

$$\int_{V_0}^{V} \frac{dV}{(U-V)^2} = \int_0^t \frac{3\rho}{8\rho_d r} C_d dt \tag{3.25}$$

If we further assume that C_d, ρ, ρ_d, and r are constant, integration yields:

$$V = U - \frac{U - V_0}{1 + \frac{3}{8}\frac{\rho}{\rho_d}\frac{1}{r} C_d (U - V_0)^2 t} \tag{3.26}$$

Equation 3.26 has the property that $V \to U$ as $t \to \infty$, which fits our original intuition that the droplet decelerates into the mean flow.

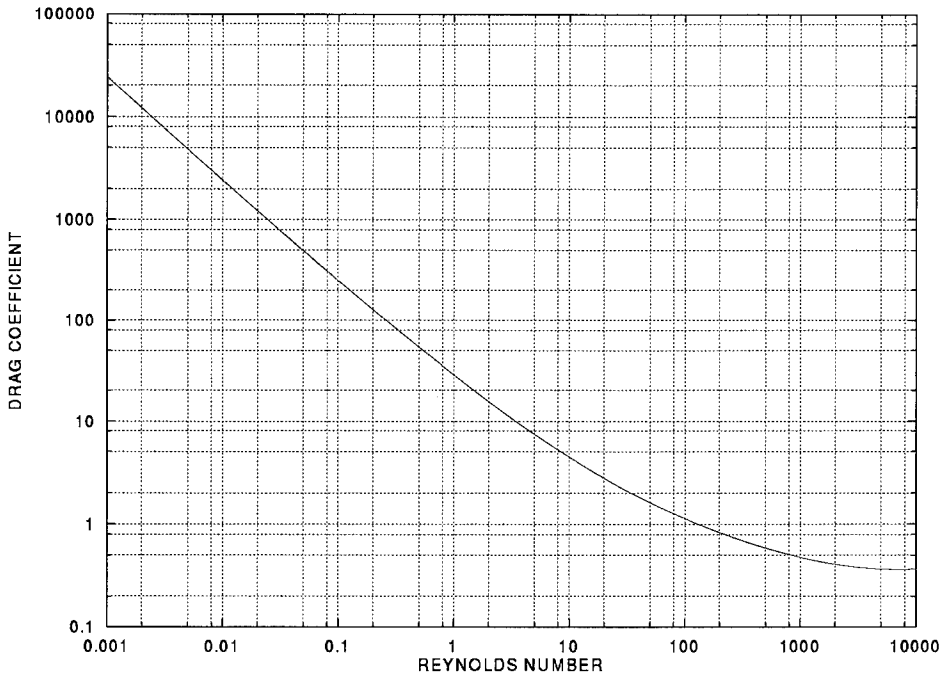

Figure 3.3 The Langmuir-Blodgett Relation for C_d vs. Re

The droplet drag coefficient is a function of the Reynolds number Re of the flow; the Reynolds number is a dimensionless ratio of inertia force to friction force, usually expressed as [28:200]:

$$Re = \frac{\rho V_{rel} L}{\mu} \tag{3.27}$$

where L is a characteristic length and μ is the kinematic viscosity of the fluid. In the case of the droplet, we take $L = D$, the diameter, so the our relation becomes:

$$Re = \frac{\rho V_{rel} D}{\mu} \tag{3.28}$$

Bilanin [4] and Teske [31] suggest a relationship between Re and C_d for spherical droplets, originally developed by Langmuir and Blodgett:

$$C_d = \frac{24}{Re}\left(1 + 0.197 Re^{0.63} + 2.6 \cdot 10^{-4} Re^{1.38}\right) \tag{3.29}$$

The relationship is depicted in Figure 3.3. Examining the order of magnitude of

terms in Equation 3.26 does not suggest that we can neglect this initial deceleration. We implement our model to account for this initial deceleration using Equation 3.26.

Once in the mean flow, droplet trajectory is computed using the component wind speeds and Δt. We note that we account for Coriolis accelerations in the droplet trajectory by assuming the droplet follows the wind.

3.6 The Dispersion Model

3.6.1 Model Description. We treat the plume of jettisoned fuel as a continuous mass distributed over a horizontal plane. The plume is modeled over a two-dimensional grid that extends beyond the physical dimension of the plume, so that there always exists a zero-concentration boundary condition on the grid. The two-dimensional diffusion equation, Equation 3.31, is solved numerically over this grid for a given time Θ using time step Δt. This Δt is independent of the time step used in the evaporation and advection model.

Figure 3.4 depicts model execution. The grid is initialized with a fixed mass at time $t = 0$, then updated at intervals of Δt; Δt may be fixed or variable, depending on the numerical scheme. After each iteration, the plume dimension is examined with respect to the grid dimension, and if the solution appears to be creeping to the edges of the grid, the grid is expanded in place. This expansion does not add points to the grid but rather doubles the step size between grid points. The current grid is embedded in a new grid nominally twice the dimension of the current grid, and so the zero-concentration boundary condition is maintained. Execution continues until $t = \Theta$.

3.6.2 Model Initialization. The grid is initialized with a plume of known mass, length and width where length is assumed to be the dominant horizontal dimension. For convenience, the plume length is aligned on the x-axis, while plume width is aligned on the y-axis.

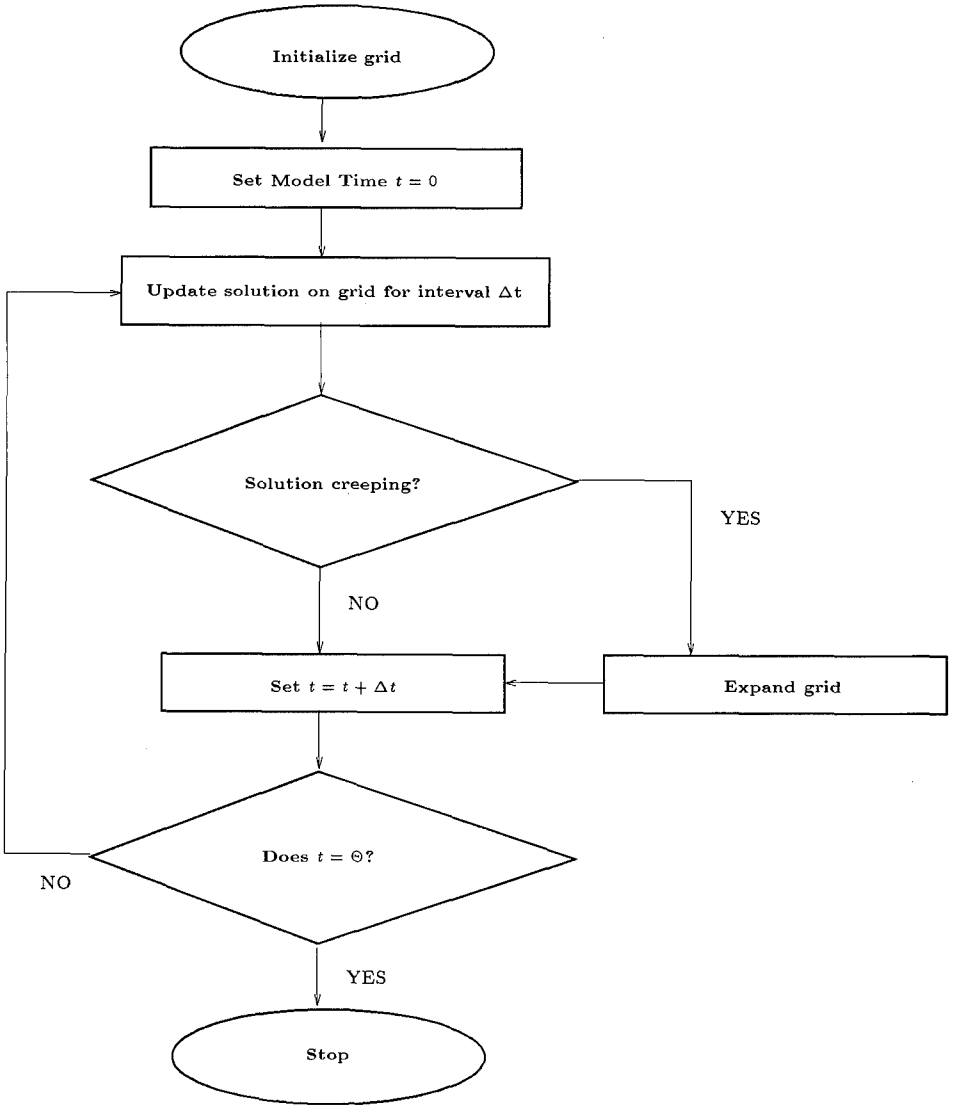

Figure 3.4 The Dispersion Model

Plume mass is distributed in a line along the y-axis so that the resulting concentration along the line has a Gaussian distribution

$$g(y) = \frac{1}{\sqrt{2\pi}\sigma} \exp\left(\frac{-(y-y_0)^2}{2\sigma^2}\right) \tag{3.30}$$

where y_0 is the coordinate of the center of the plume and nominally

$$\sigma = \frac{\text{plume width}}{3}$$

Distribution along the x-axis is uniform over most of the plume length, with short (approximately 10% of plume length) "ramp-up" and "ramp-down" distributions at the ends of the plume. These adjustments to the ends of the plume are made to facilitate a smoother numerical solution; similarly, the assumption of a Gaussian distribution along the plume width is convenient. Although we do not have experimental evidence to formulate precisely these initial conditions, we do know qualitatively that we can consider our plume as a line source. Our Gaussian initial conditions are consistent with steady-state, continuous source solutions for a line source (see, for example, Seinfeld [27:600] or Hanna [15:51–52]). We conclude that our initial conditions are representative of the initial release and distribution of the aviation fuel.

3.6.3 Model Physics. We model the distribution of concentration over the grid using a simplified form of the Fickian or K-theory diffusion equation (see, for example, Seinfeld [27:522] or Zannetti [34:107]):

$$\frac{\partial c}{\partial t} = K_x \frac{\partial^2 c}{\partial x^2} + K_y \frac{\partial^2 c}{\partial y^2} \tag{3.31}$$

where c is the ensemble-averaged or mean concentration and K_x and K_y are the eddy diffusion coefficients. This treatment assumes that molecular diffusion is negligible and that the primary mechanism affecting concentration is atmospheric turbu-

lence, parameterized in K_x and K_y [27:522–523]. We conclude that c is not affected by changes in mass and so we are justified in treating dispersion separately from evaporation. Advection, often incorporated into the diffusion equation, is already considered in a separate model. Strikwerda, in particular, has demonstrated that advection and dispersion in a fixed reference frame are equivalent to dispersion in an advected reference frame [30:114].

We are interested in the deposition concentration (mass per area) at ground fall. We deliberately choose a two-dimensional reference frame for our plume, assuming that vertical dispersion is negligible and that, similar to our advection model, our plane is located through the center of mass of the plume [27:534]. We assume, then, that when the droplet makes ground fall the plume strikes the ground; that is, all mass in the column above the droplet simultaneously makes ground fall.

To calculate a numerical solution to Equation 3.31 we employ two different grid techniques. We adapt a Fourier series solution to our grid in a method similar to an analytical derivation presented by Seinfeld [27:553]. To verify results from this Fourier technique, we also implement a finite difference solution.

3.6.4 Numerical Methods.

3.6.4.1 Fundamental Relations. We begin with Equation 3.31 and assume boundary and initial conditions:

$$c(x, y, 0) = p(x)q(y)$$
$$c(x, y, t) \to 0 \text{ as } x, y \to \pm\infty$$

This initial condition implies that the initial distribution is separable in x and y. We assume further that we can separate $c(x, y, t)$ into $c = f(x, t)g(y, t)$, so that

Equation 3.31 becomes two partial differential equations

$$\frac{\partial f}{\partial t} - K_x \frac{\partial^2 f}{\partial x^2} = 0 \tag{3.32}$$

where

$$f(x,0) = p(x)$$
$$f(x,t) \rightarrow 0 \text{ as } x \rightarrow \pm\infty$$

And

$$\frac{\partial g}{\partial t} - K_y \frac{\partial^2 g}{\partial y^2} = 0 \tag{3.33}$$

where

$$g(y,0) = q(y)$$
$$g(y,t) \rightarrow 0 \text{ as } y \rightarrow \pm\infty$$

If f satifies Equation 3.32 and g satisfies Equation 3.33, and $c = fg$, then c satisfies Equation 3.31. By the uniqueness theorem this is the only solution for c (for a brief discussion see Sommerfeld [29:82–83] or Arfken [2:79]). We note the similarity of Equation 3.32 to Equation 3.33 and continue our analysis with $f(x)$. This same analysis applies to $g(y)$, the solution of Equation 3.33.

3.6.4.2 Iterative Fourier Solution. To effect a Fourier solution of Equation 3.32, we first transform the initial and boundary conditions so that

$$f(x,0) = p(x) \text{ for } 0 < x < L$$
$$f(0,t) = f(L,t) = 0$$

The solution, then, is

$$f(x,t) = \Sigma_{n=1}^{\infty} A_n \sin\left(\frac{n\pi x}{L}\right) \exp\left(\frac{-K_x n^2 \pi^2}{L^2} t\right) \tag{3.34}$$

where

$$A_n = \frac{2}{L} \int_0^L p(x) \sin \frac{n\pi x}{L} dx \tag{3.35}$$

This is a common result; see, for example, Burden and Faires [7:566–567] or Boas [6:543–547]. We could calculate our solution directly with this treatment, setting $t = \Theta$, the total time of descent, to arrive at the concentration distribution at the ground. We can only calculate a finite number of terms, however, and with Θ on the order of an hour to ten hours, we could not carry enough Fourier terms to get a reasonably accurate solution. Such a one-step solution is particularly bad if the plume grows to exceed L at $t = \Theta$, because this situation violates zero boundary conditions. We instead incorporate this Fourier solution into an iterative scheme.

The iterative solution uses m time steps such that $\Theta = m\Delta t$, where Δt is chosen empirically as a compromise between accuracy and time. At each time step, new Fourier coefficients (nominally 60 to 80) are calculated using the trapezoid rule to integrate Equation 3.35 over the grid, so the previous time step's $f(x)$ becomes the following time step's $p(x)$.

Zero-concentration boundary conditions are initialized by embedding the plume dimension d (referring either to width or length) in the center of a grid line of length $3 \cdot d$. These boundary conditions are maintained by examining solution creep after every iteration. Solution creep is determined by comparing plume dimension to grid length. Plume dimension is defined to be the line that contains the set of all concentration values greater than $0.001 f_{max}$ where f_{max} is the maximum concentration in the plume line. The threshold, set empirically, is

$$\frac{\text{plume dimension}}{\text{grid line length}} > 0.67$$

That is, if the plume dimension has crept to two-thirds of the grid line, the grid must be expanded in place to maintain zero boundary conditions.

3.6.4.3 Finite Difference Solution. To formulate a finite difference solution, we rewrite Equation 3.32 using a first-order forward-difference approximation to the time derivative (i subscript) and a second-order center-difference for the

space derivative (j subscript):

$$\frac{c_{i+1,j} - c_{i,j}}{\Delta t} = K_x \frac{c_{i,j+1} - 2c_{i,j} + c_{i,j-1}}{\Delta x^2} \tag{3.36}$$

This can be written as an explicit solution for $c_{i+1,j}$, thus:

$$c_{i+1,j} = c_{i,j} + \frac{K_x \Delta t}{\Delta x^2} (c_{i,j+1} - 2c_{i,j} + c_{i,j-1}) \tag{3.37}$$

While easy to implement, this forward-time center-space formulation is not stable unless [30:120]

$$\Delta t \leq \frac{\Delta x^2}{2K_x} \tag{3.38}$$

This stability condition forces a smaller time step to achieve a more accurate grid representation (smaller Δx). This scheme is second-order accurate in space, and by formulation first-order accurate in time. Satisfying this stability condition, however, makes the scheme second-order accurate in time [30:120].

3.6.5 Eddy Diffusion Parameters. Implicit in our numerical solution is a scheme to calculate the eddy diffusion coefficients K_x and K_y. Zannetti [34:125–130], Seinfeld [27:597–598], and Hanna [15:50–56] present extensive discussions on calculating horizontal diffusion parameters for specific solutions to Equation 3.31 and the general advection-diffusion equation.

Eddy diffusion is typically parameterized in terms of conveniently measured (or estimated) quantities [15:27]. We have wind and temperature data along the droplet descent through the environmental model. From this data we can infer the variability of the wind, then approximate the eddy turbulence parameters K_x and K_y. Zannetti offers the following relation for long-range transport and diffusion from a point source [34:128]:

$$K_h = \frac{10^3 \sigma_\theta^2 u}{2} \tag{3.39}$$

where

σ_θ = standard deviation of the horizontal wind in radians

u = mean wind speed in m/s

Zannetti [34:128] develops Equation 3.39 based on work by Irwin. Hanna [15:31] presents a similar result with reference to Irwin. Zannetti notes that this relation results in dispersion parameters an order to two orders of magnitude smaller than the low end of the range of experimentally derived parameters (10^2 to 10^3 versus 10^4 to 10^7 m^2/s [34:128]. Experimentally derived parameters, however, necessarily incorporate the variability of measurements; Zannetti accounts for the anomalously small K_h from Equation 3.39 in the uncertainty of the meteorological diagnosis or prognosis of the wind field [34:128]. In examining uncertainty in air quality models, Lewellen [20] used an estimate of uncertainty in rawinsonde wind measurements that varied from $\pm 5°$ at 10 m/s to $\pm 180°$ under calm conditions. We take the observed deviation in wind direction as σ_θ, and take the deviation in wind direction due to meteorological uncertainty as σ'_θ. Using Lewellen's uncertainty estimation, we fit an exponential function for σ'_θ over the range of wind speeds less than 10 m/s, so that:

$$\sigma'_\theta = \pi \exp(-0.367u) \tag{3.40}$$

where we expect u in meters per second and return σ'_θ in radians. Finally, we substitute into Equation 3.39 the term $\Delta\theta$ for σ_θ, where

$$\Delta\theta = \sigma_\theta + \sigma'_\theta \tag{3.41}$$

With a single vertical profile, we cannot directly calculate σ_θ; we approximate this quantity at altitude z by examining the variability of the wind through a layer centered (vertically) at z. The x-axis is, by design, along the release heading of the aircraft ϕ, and so the y-axis must be along the heading $\phi + 90°$. If we define θ to be

the mean wind direction at altitude, our eddy diffusion parameters are:

$$K_x = \frac{10^3 \Delta\theta^2 u \mid \cos(\phi - \theta) \mid}{2} \tag{3.42}$$

and

$$K_y = \frac{10^3 \Delta\theta^2 u \mid \cos(90° - \phi - \theta) \mid}{2} \tag{3.43}$$

Although we note that

$$\mid \cos(90° - \phi - \theta) \mid = \mid \sin(\phi - \theta) \mid$$

the similarity in form of Equations 3.42 and 3.43 are a better generalization for computation.

3.7 Summary

We have presented our proposed solution to the problem of determining the fate of jettisoned fuel. We perceive this original problem as two problems: determining the fate of fuel droplets, and determining the fate of the aggregate plume. We have presented an evaporation and advection model to predict the fate of fuel droplets, and a dispersion model to predict the final distribution of the plume. In complement to these active models, we have presented an environmental model to better characterize the atmosphere during a jettison event.

IV. Model Results

4.1 Overview

We now present results developed with the implementation of our model design. We first examine individual model components to demonstrate agreement of our implementation with previous work. We then provide supporting evidence for physical assumptions in the overall model design (e.g. neglecting plume tilt). We conclude with sample results from the integrated model, comparing predicted ground level contamination with calculations from Clewell [8].

4.2 Verification of the Evaporation Model

4.2.1 Introduction. To confirm that our evaporation model is implemented correctly, we compared current model output with Clewell's published results. Using case studies predicting the fate of individual fuel droplets and distributions of droplets, we demonstrated reasonable agreement with Clewell's original calculations. In verifying our model against this previous work we used the published fuel component models [11:5–7] for JP-4, JP-8, and DF #2. These fuel models are detailed in Tables A.1, A.2 and A.3 of this thesis.

4.2.2 Fate of Individual Droplets. Clewell reported four case studies using separate evaporation calculations [8:108–113]. These results, along with our current results, are summarized in Table 4.1. Release altitude for all cases was 1500 meters; release airspeed was 175 meters per second (m/s) or approximately 350 knots. We reproduced these previous results to within 5% of the original numbers. We note that Clewell's work was accomplished in 1979-80, using single-precision arithmetic in FORTRAN IV; the computer architecture is unspecified [8:97–102]. We implemented our model using double-precision arithmetic in ANSI C on an i486 architecture.

Fuel: JP-4 Release altitude: 1500 m Release airspeed: 175 m/s						
Case	Initial Diameter (microns)	Surface Temperature (Celsius)		Time of Fall (minutes)	Percentage Mass Remaining	Final Diameter (microns)
1	270	20.0	Clewell	684.613	0.13	25
			Current	684.650	0.13	25
2	270	0.0	Clewell	131.241	1.77	65
			Current	131.362	1.80	65
3	270	-20.0	Clewell	52.267	10.66	123
			Current	52.163	11.00	125
4	500	0.0	Clewell	27.848	5.48	181
			Current	27.826	5.76	184

Table 4.1 Predicted fate of individual droplets

Given the iterative nature of the calculations, these differences in implementation may account for the observed differences in results.

4.2.3 Ground Contamination from a Droplet Distribution. Clewell characterized the plume of jettisoned fuel as a distribution of droplets; ground contamination was predicted by considering the contribution (in terms of a mass weight) of each droplet to the final liquid fuel ground fall [11]. We adapted our evaporation model code to consider a distribution of droplets to facilitate comparison with Clewell's case studies. This droplet distribution is depicted in Figure 4.1. Our composite model data were collected by using this distribution of droplets at 33 temperatures in the range -40°C to 40°C (data points taken at intervals of 2 to 3 C°). As in Clewell's study, release altitude was 1500 meters; release airspeed was 175 m/s [8:108–113]. Consistent with the original study, we examine JP-4, JP-8, and DF #2. We reproduce Clewell's original summary in Figure 4.2. Data from our model is summarized in Figure 4.3. We observed excellent agreement between Clewell's results and our current results.

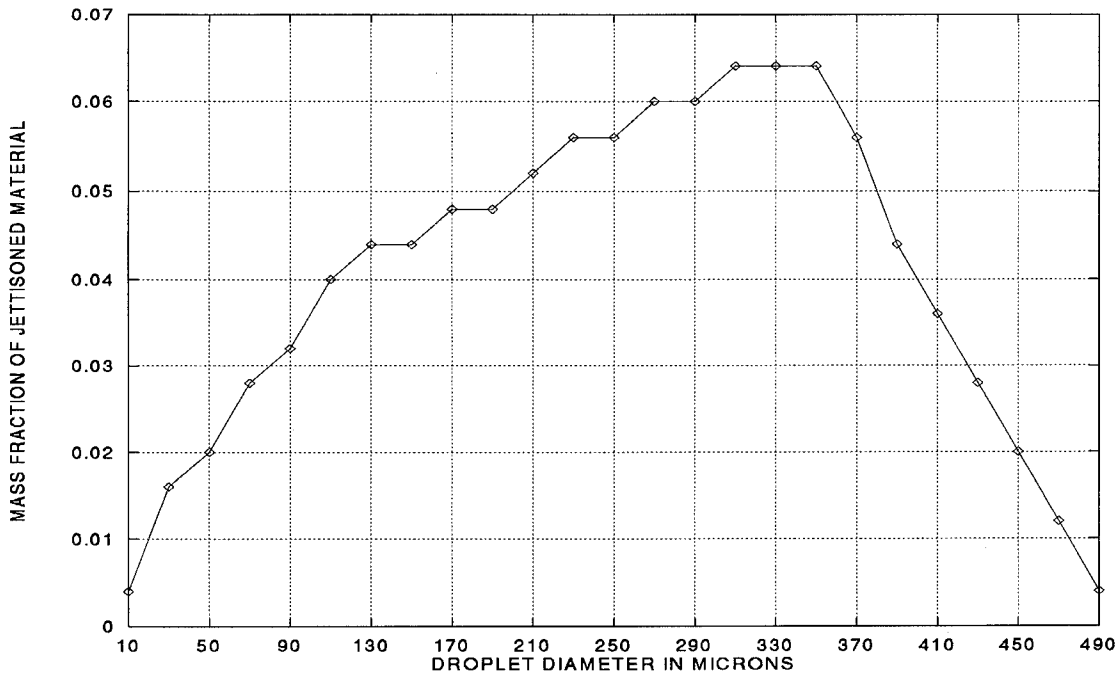

Figure 4.1 Clewell's Droplet Distribution [8:108]

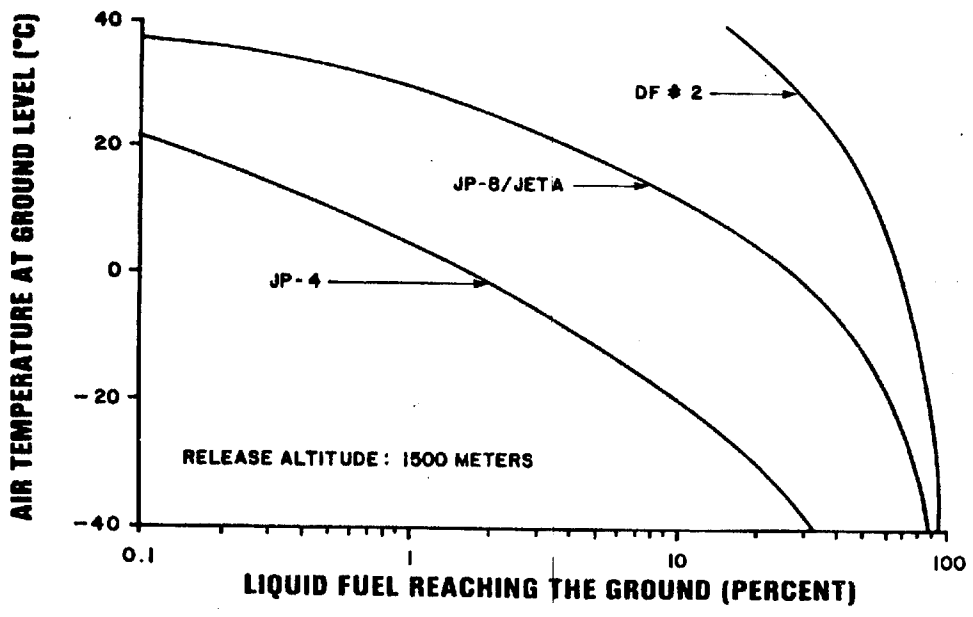

Figure 4.2 Reprinted from Clewell [11:17]

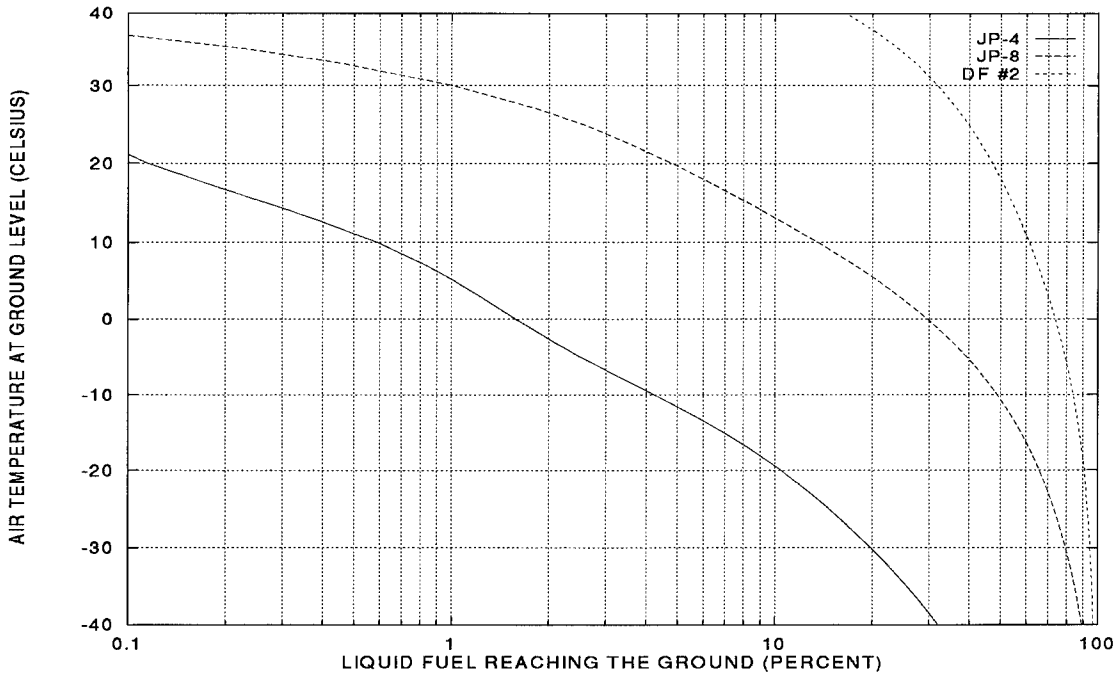

Figure 4.3 Current model results using a droplet distribution

4.3 Validity of the Single-Droplet Model

Although our evaporation model is capable of generating data from a distribution of droplets, we have made the simplifying assumption that we can represent the plume of jettisoned fuel as a homogenous distribution of droplets, nominally 270 microns in diameter. We offer supporting evidence for this assumption by comparing predicted ground contamination from a single droplet to the prediction for a droplet distribution.

We have demonstrated that our evaporation model reproduces Clewell's original results in predicting the amount of liquid fuel remaining at ground fall. Using the same temperature data points as in Section 4.2.3, we performed our calculations using a single droplet with a diameter of 270 microns, a release altitude of 1500 meters, and a release airspeed of 175 m/s. Results for JP-4, JP-8 and DF #2 are presented in Figures 4.4, 4.5 and 4.6. We observed qualitatively that for colder temperatures the single droplet assumption overestimates ground fall while at warmer

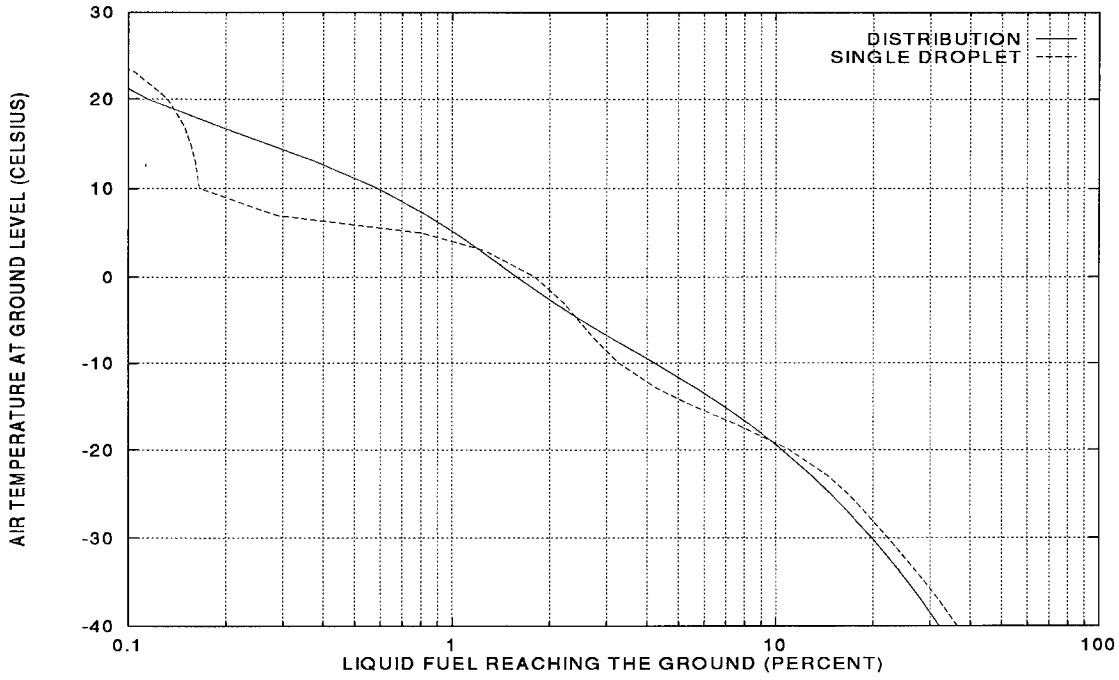

Figure 4.4 Single droplet results for JP-4

temperatures this assumption appears to underestimate ground fall. At warmer temperatures, however, this error is less significant because the overall amount of liquid fuel remaining is smaller. Quantitatively, we observed that the mean error for JP-4 is 0.88%, for JP-8, 4.63% and for DF #2, 6.21%. We conclude that our single droplet assumption is valid.

4.4 Neglecting Plume Tilt

In Section 3.2.3 we presented preliminary analysis to support neglecting plume tilt in model calculations. To confirm this analysis, we present model results following two tracer droplets, one released in the trailing edge of the plume and the other released in the leading edge. We follow the distance between these droplets from release to ground fall of the leading edge (last released) droplet. We take as the actual plume length the three-dimensional distance between these droplets.

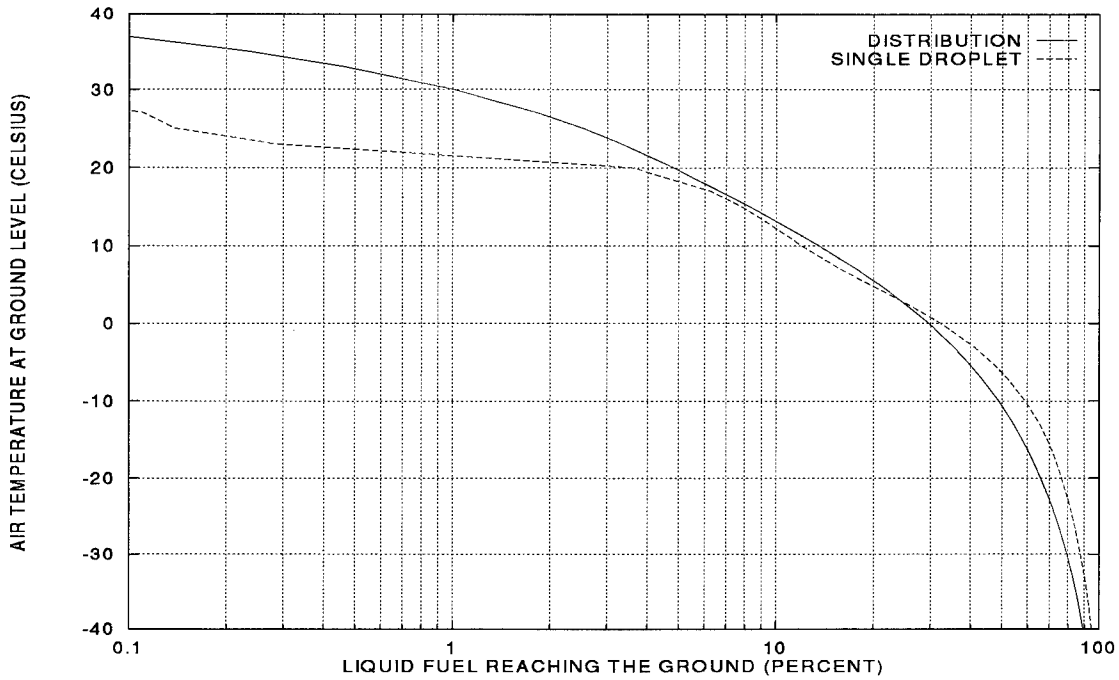

Figure 4.5 Single droplet results for JP-8

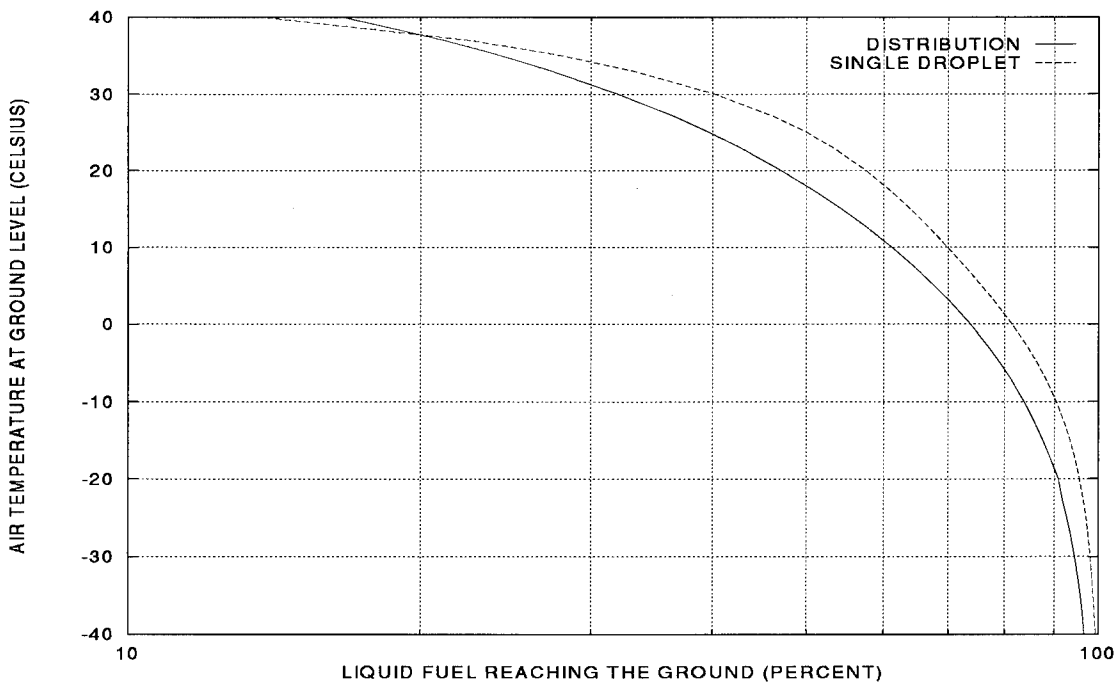

Figure 4.6 Single droplet results for DF #2

Recalling our analysis in Equations 3.4 and 3.6, we assumed that the worst-case error condition is a release downwind so that the plume is stretched initially, descending into a strong surface wind so that the plume is further stretched at ground fall. Note that we define "worst-case" here to mean the largest error in results; by neglecting plume stretch in this scenario, we obtain more conservative (i.e. overestimated) ground contamination results. We also suspected that a slower release airspeed will increase the error in neglecting plume tilt. We used our single-droplet model (with mean diameter 270 microns) and complete model runs at release airspeeds of 100, 175, and 250 m/s, all downwind. We assume a uniform wind speed of 10 m/s from release altitude (1500 meters) to surface. To investigate the dependence of plume length error ϵ on the ratio of initial and final terminal velocity, we performed calculations at -20°C, 0°, and 20°. Of these 27 cases, we find that plume length errors are bounded by $\epsilon < 10^{-4}$ at ground fall. These errors were largest for release airspeed $V_a = 100$ m/s, and we present these cases in Figures 4.7, 4.8 and 4.9. The noticeable "kinks" in these graphs represent the point at which the trailing edge droplet made ground fall. Although we predicted that warmer temperatures would increase the ratio of initial terminal velocity to final terminal velocity, this effect seems minor compared to the effect of release airspeed; we observe that within the cases for $V_a = 100$ m/s, JP-4 experienced the greatest error in plume length at ground fall, though this difference compared to JP-8 and DF #2 under the same conditions appears smaller than the difference in results from cases at $V_a = 175$ m/s and $V_a = 250$ m/s.

4.5 Magnitude of Initial Droplet Deceleration

In formulating our advection model, we did not negelect the initial droplet deceleration into the mean wind because our analysis did not indicate positively that this error would be negligble. Model results using this deceleration code, however, suggest that the droplet displacement due to this initial deceleration is very small

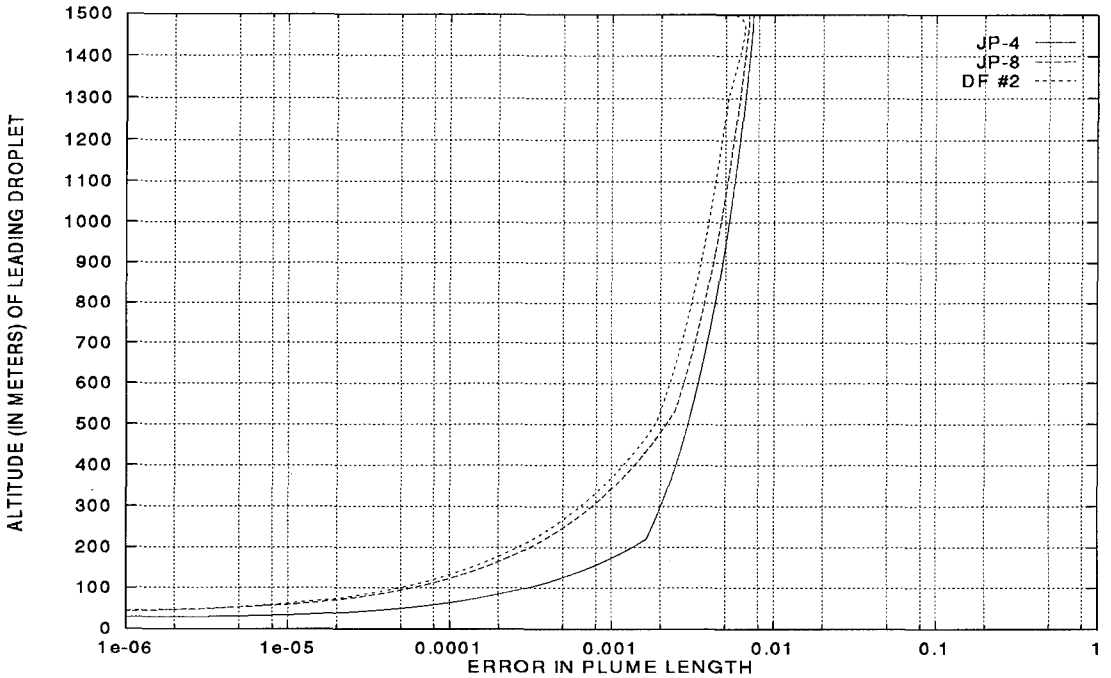

Figure 4.7 Plume tilt error, $V_a = 100$ m/s, $T_0 = -20°$

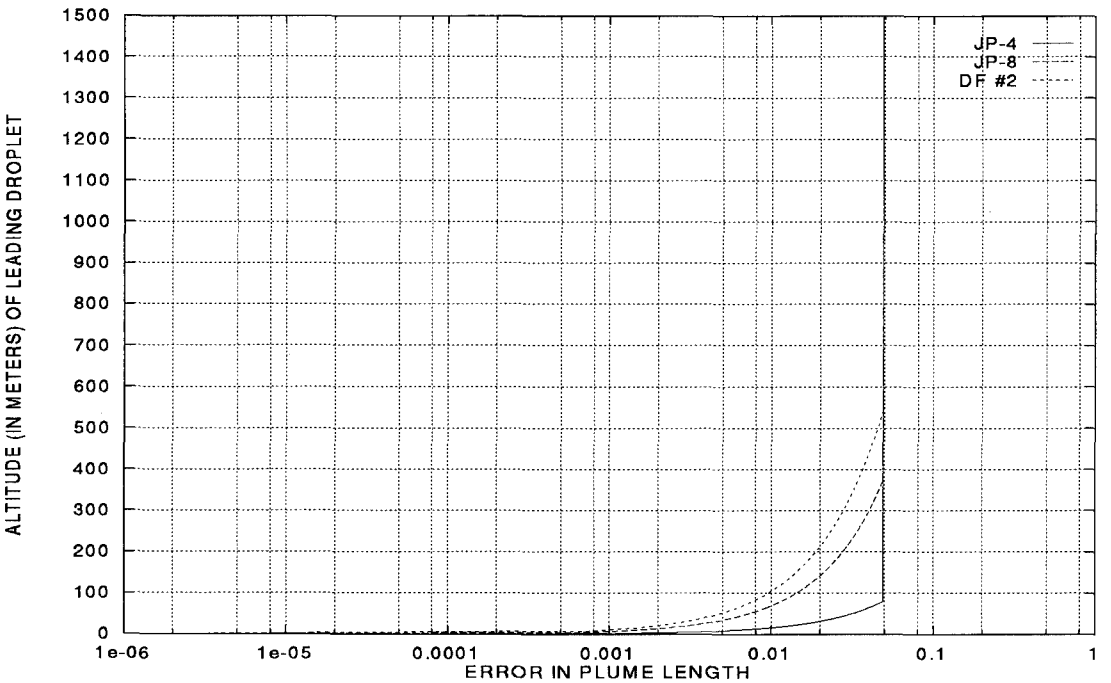

Figure 4.8 Plume tilt error, $V_a = 100$ m/s, $T_0 = 0°$

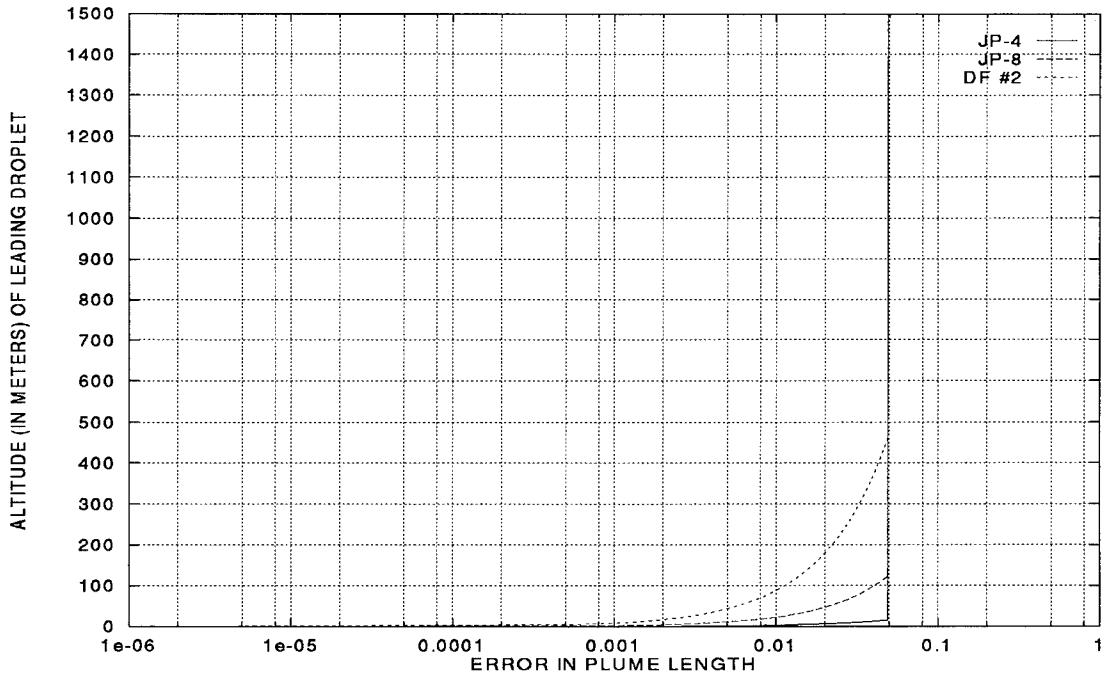

Figure 4.9 Plume tilt error, $V_a = 100$ m/s, $T_0 = 20°$

relative to the total translated distance. We used the droplet distribution detailed in Table 4.1 and calculated with zero wind speed so that any droplet displacement could be attributed to this deceleration. Model results were generated for release airspeeds of 100, 175, and 250 m/s or 200, 350, and 500 knots respectively, using surface temperatures of -20°C, 0°, and 20°C.

Reviewing the data from these calculations, we observed the following trends. The fuel DF #2 requires more time to decelerate under all release speeds and environmental conditions investigated. Given the low evaporation rate of this fuel under most conditions, the droplet diameter, and so the corresponding drag coefficient, changed very little. The more volatile JP-4 and JP-8 droplets evaporate, decreasing in diameter, in turn decreasing the Reynolds number (Equation 3.28) and increasing the droplet drag coefficient C_d (Figure 3.3). Of the three release speeds investigated, $V_a = 100$ m/s appears to require the longest deceleration time (see Figures 4.10 and 4.11), and therefore produces the largest droplet displacement, at all temperatures

and for all fuels examined. Given that the drag force is proportional to the relative airspeed (see Equation 3.22), this result seems reasonable.

To assess the potential error were we to neglect this initial deceleration, we first observe that the typical time scale Θ for our model is one to ten hours, or 10^3 to 10^4 seconds. Assuming a light mean wind from jettison altitude to surface at 1 m/s, the droplet will translate a distance of 10^3 to 10^4 meters. We present model output from two of the cases in Figures 4.10 and 4.11, a typical case at airspeed $V_a = 175$ m/s and surface temperatures $T_0 = 20°C$ and an extreme case at $V_a = 100$ m/s and $T_0 = -20°C$. Model output is shown for a distribution of droplets. Taking the mass median diameter of 270 microns, for a typical release (Figure 4.10) neglecting the initial deceleration causes a position error of 17 meters or at most 1.7% for DF #2, 8.6 meters or 0.86% for JP-8, and 2.3 meters or 0.23% for JP-4. In the extreme case of slow release speed and cold atmosphere (Figure 4.11), these errors increase to 167 meters for DF #2, 20 meters for JP-8, and 3.6 meters for JP-4.

In these extreme cases, the 270 micron droplet decelerates into the mean wind within 0.04 minutes of release for JP-4, within 5.67 minutes for JP-8, and with 13.67 minutes for DF #2. We conclude that we could normally neglect this initial deceleration in calculating droplet position. Atmospheric and release conditions do exist in which the position error may be large, however, and these conditions (i.e. cold atmosphere) are precisely those in which we are most concerned about ground contamination. We decide, then, to maintain this deceleration calculation in the integrated model. Given the short time to decelerate for JP-4 and JP-8, we conclude that the computational cost incurred is small.

4.6 Representative Meteorology

4.6.1 Overview. We introduce representative meteorology into the integrated model by means of the passive environmental model. Although we did not perform an exhaustive study of the effect of different meteorological conditions on

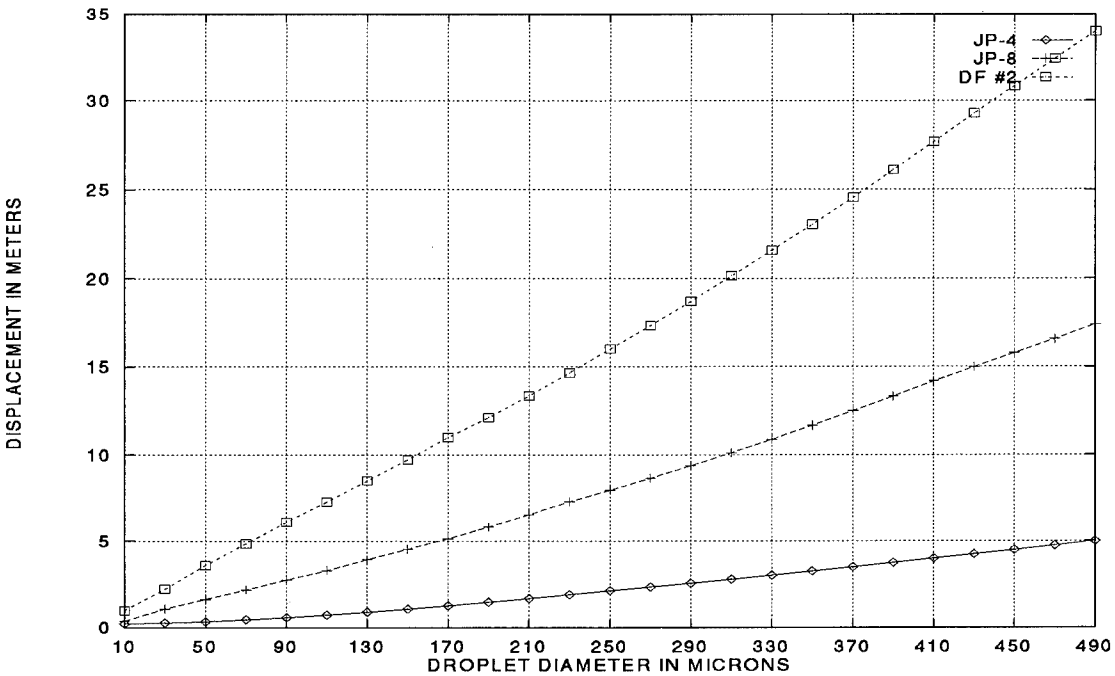

Figure 4.10 Displacement due to deceleration ($V_a = 175$ m/s, $T_0 = 20°$C)

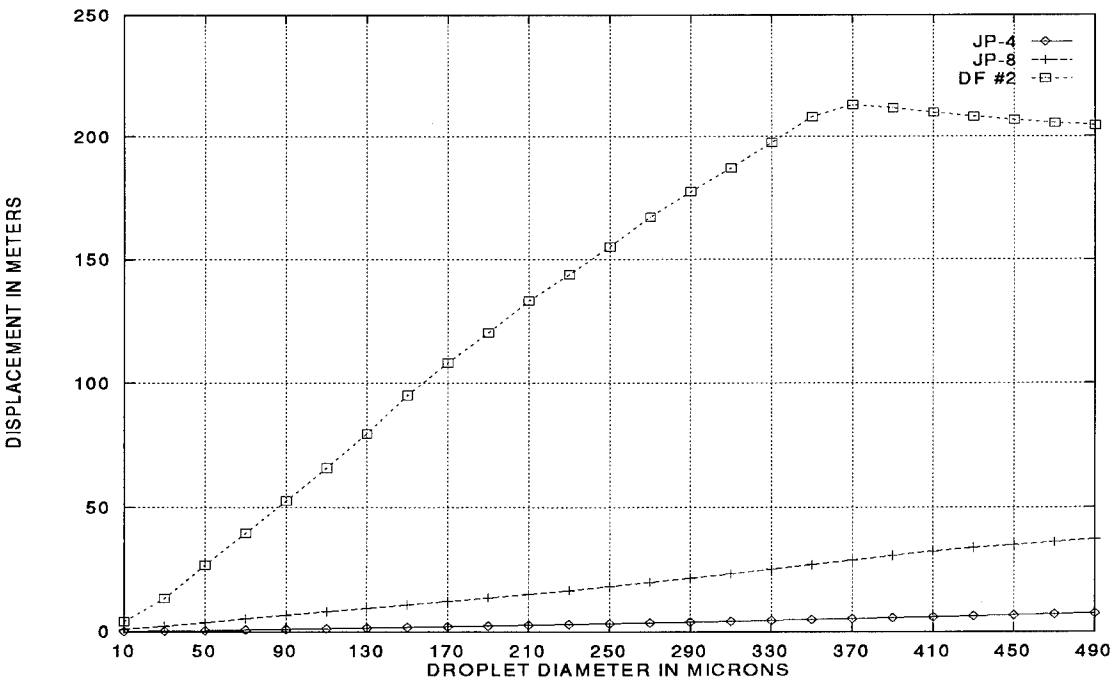

Figure 4.11 Displacement due to deceleration ($V_a = 100$ m/s, $T_0 = -20°$C)

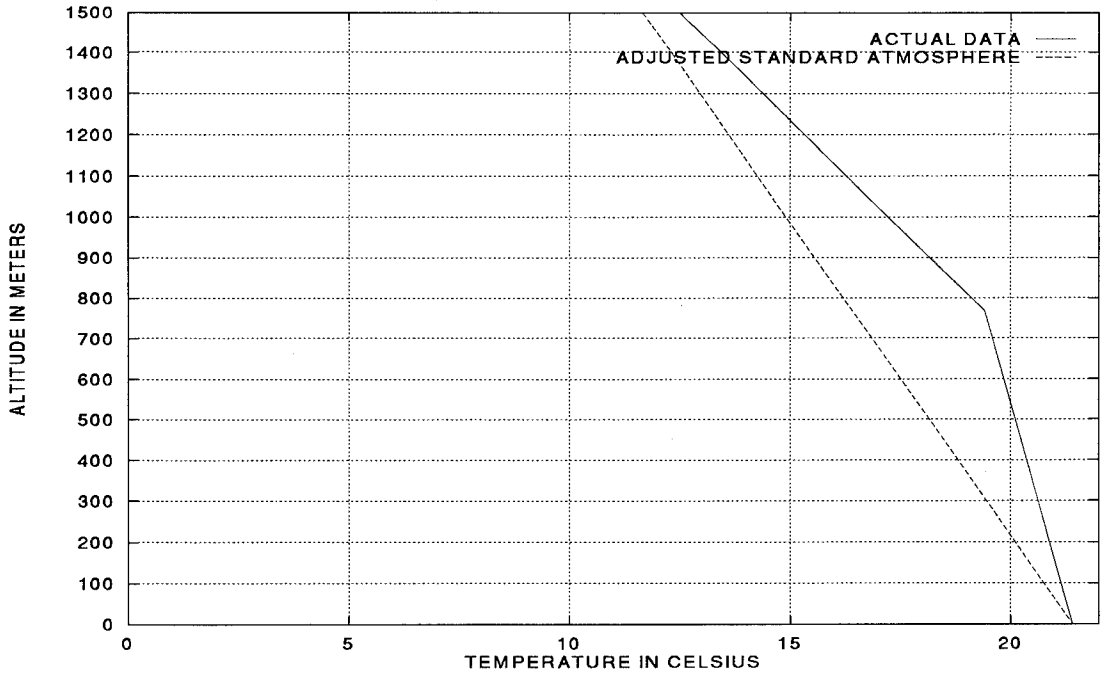

Figure 4.12 Spokane (1 Oct 94/0000 UTC) and standard profile

the overall simulation, we present sample cases that demonstrate the utility of this model. We conducted a brief study using upper air data from Spokane, Washington, for 1 October 1994, 0000 UTC, and Dayton, Ohio, for 1 October 1994, 1200 UTC. We compared these actual temperature profiles to adjusted standard atmospheres at the same surface temperatures. We used a release altitude of 1500 meters and an airspeed of 175 m/s to generate results for JP-4, JP-8, and DF #2. Consistent with our integrated model we assumed a mean diamter of 270 microns. Because we do not have a standard wind profile in the same sense that we have a standard atmosphere, we limit our comparison to the differing temperature profiles and the resulting differences in liquid fuel ground fall.

4.6.2 Spokane, WA. The Spokane data show a surface temperature of 21.4°C; we created a standard atmosphere profile adjusted to this temperature using the **makestd** utility (see Appendix D). The actual and standard temperature profiles are detailed in Figure 4.12. We see that the actual temperature profile at Spokane

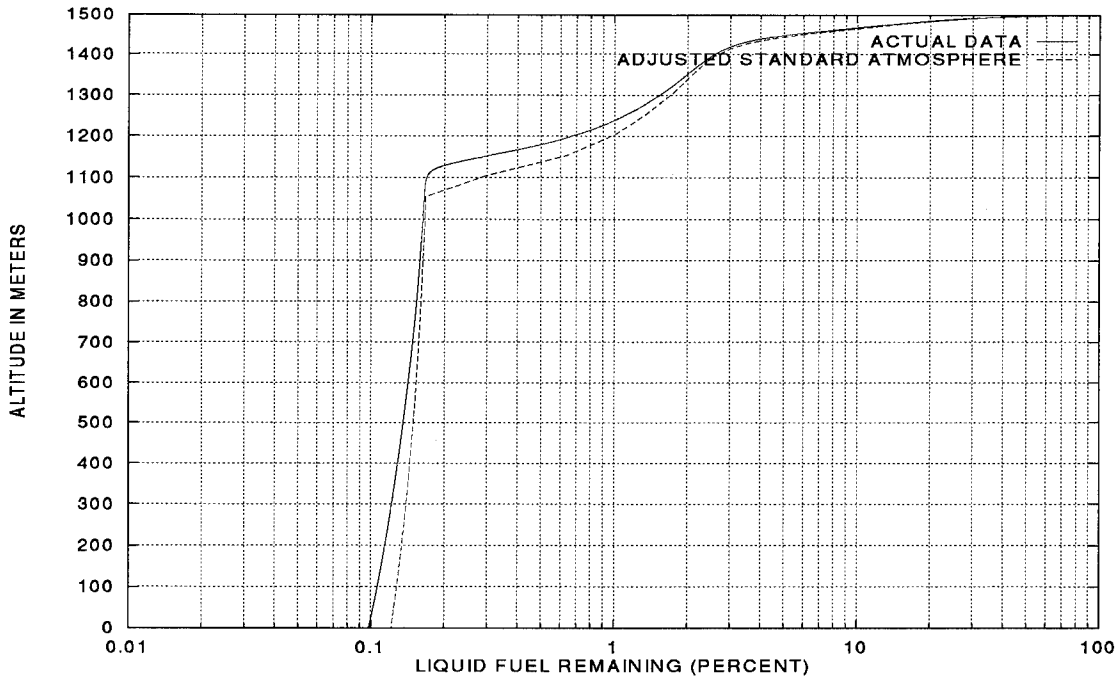

Figure 4.13 Spokane study, JP-4 ground fall

is much warmer than the standard profile throughout the layer from 1500 meters to surface. Evaporation results are depicted in Figures 4.13, 4.14, and 4.15. We observe that for the relatively volatile JP-4 and relatively involatile DF #2 this warmer temperature profile does not significantly effect the amount of fuel making ground fall. We surmise that the general state of the atmosphere is warm, and so the JP-4 evaporates readily in both profiles. We have already observed that DF #2 does not readily evaporate around 20°C, and so the temperature difference between profiles does not significantly effect the evaporation rate. For JP-8, however, we observe an order of magnitude difference between predicted ground fall from a standard atmosphere (2.11%) and the actual profile (0.15%).

4.6.3 Dayton, OH. The profile at Dayton on 1 October 1994, 1200 UTC, shows a deep surface inversion approximately 450 meters in depth (see Figure 4.16). With this inversion, the actual profile is much warmer than the standard profile. Consistent with the Spokane study, we find that the predicted ground fall for JP-

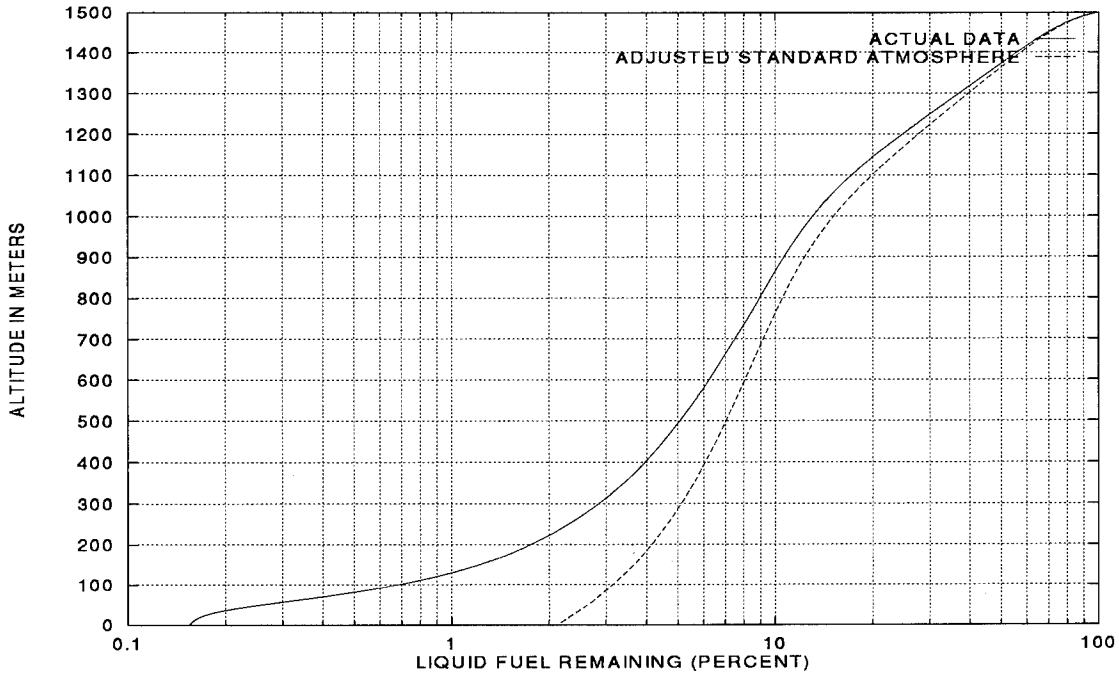

Figure 4.14 Spokane study, JP-8 ground fall

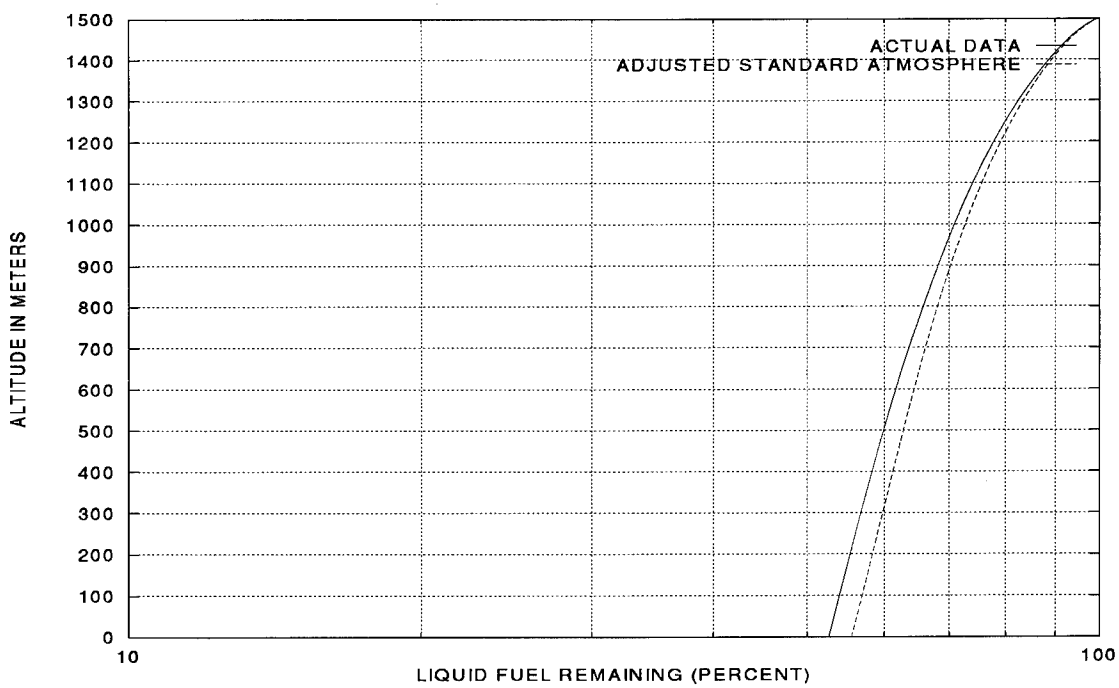

Figure 4.15 Spokane study, DF #2 ground fall

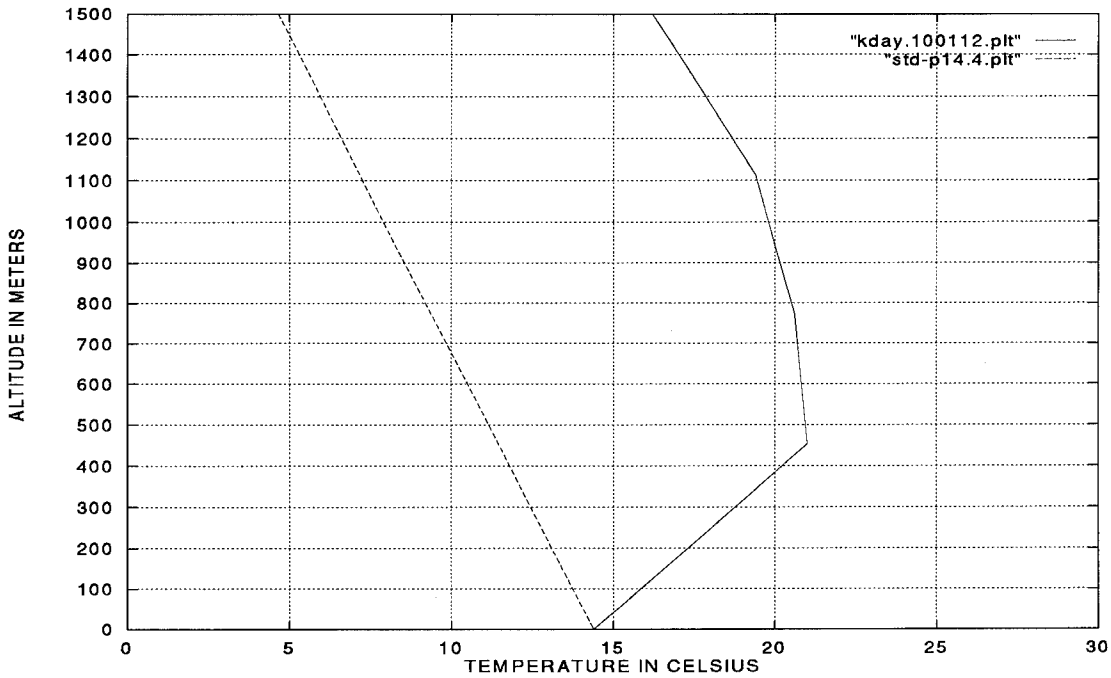

Figure 4.16 Dayton (1 Oct 94/1200 UTC) and standard profile

Fuel	Spokane		Dayton	
	Actual Profile	Standard Profile	Actual Profile	Standard Profile
JP-4	819.7	728.9	918.5	503.4
JP-8	130.7	78.7	212.8	54.8
DF #2	30.7	30.4	31.6	28.8

Table 4.2 Ground fall times (in minutes) from Spokane and Dayton studies

4 and DF #2 are only mildly affected by the differences in temperature profiles. Calculations with JP-8 using the standard profile, however, overpredicted ground fall by almost two orders of magnitude, 8.5% in contrast to the actual profile prediction of 0.15%. Ground fall predictions are summarized in Figures 4.17, 4.18, and 4.19.

4.6.4 Conclusions. Although we do not examine advection in this study, we do note that predicted time to ground fall increased under the warmer temperature profiles. These results are presented in Table 4.2. The large differences in predicted ground fall times for JP-4 and JP-8 represent significant periods (10^3

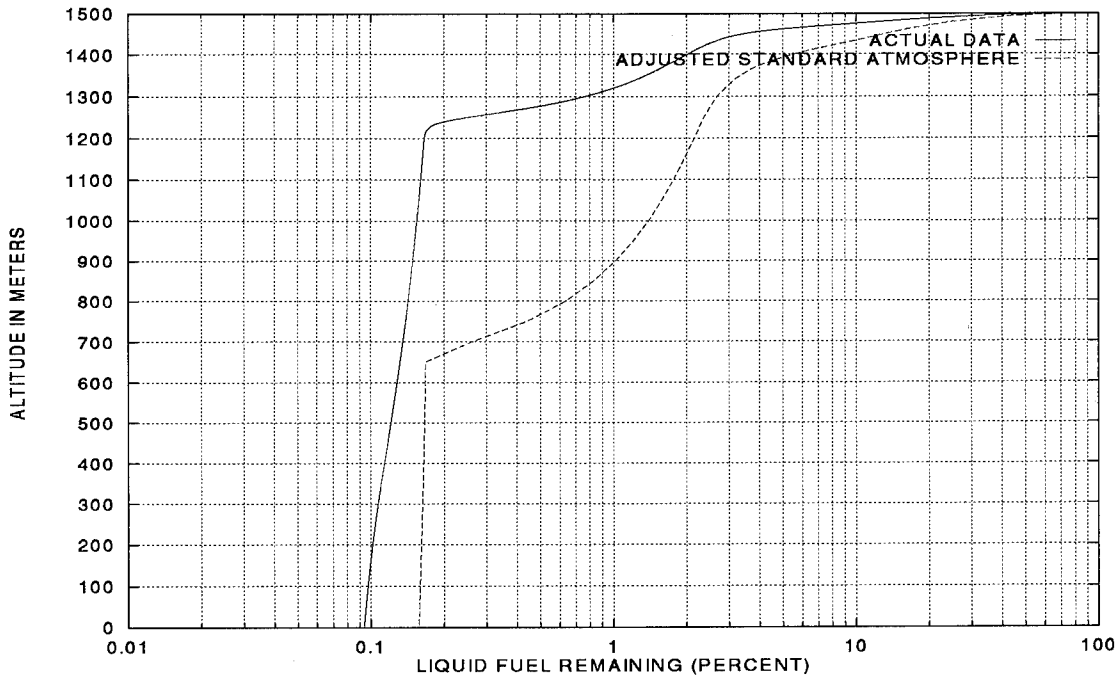

Figure 4.17 Dayton study, JP-4 ground fall

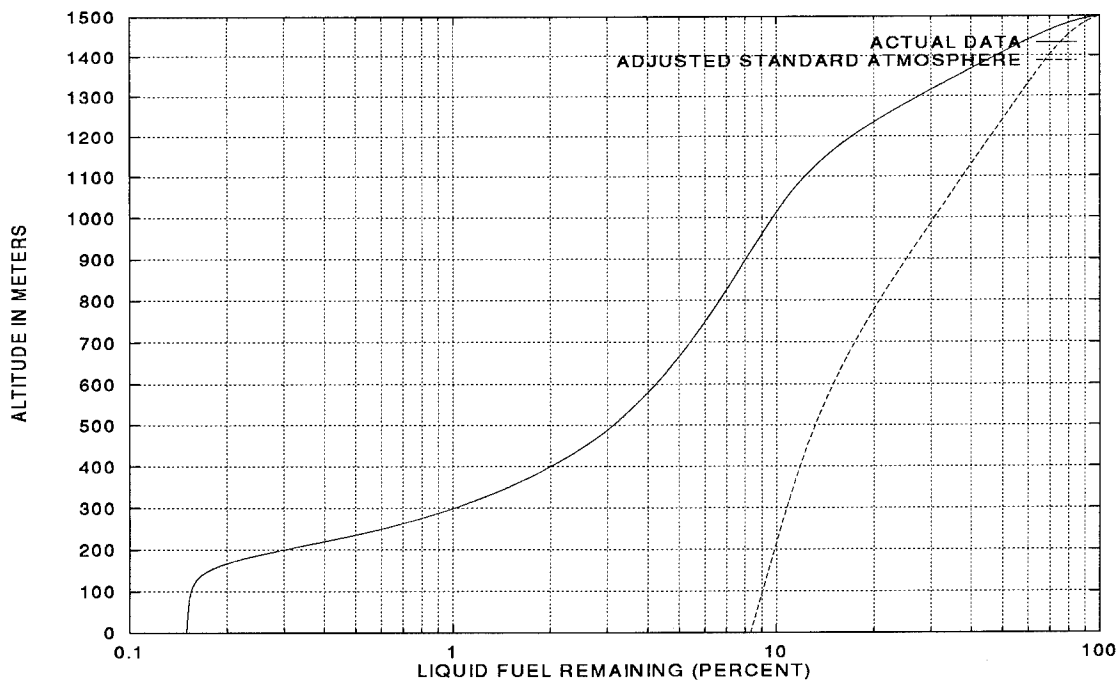

Figure 4.18 Dayton study, JP-8 ground fall

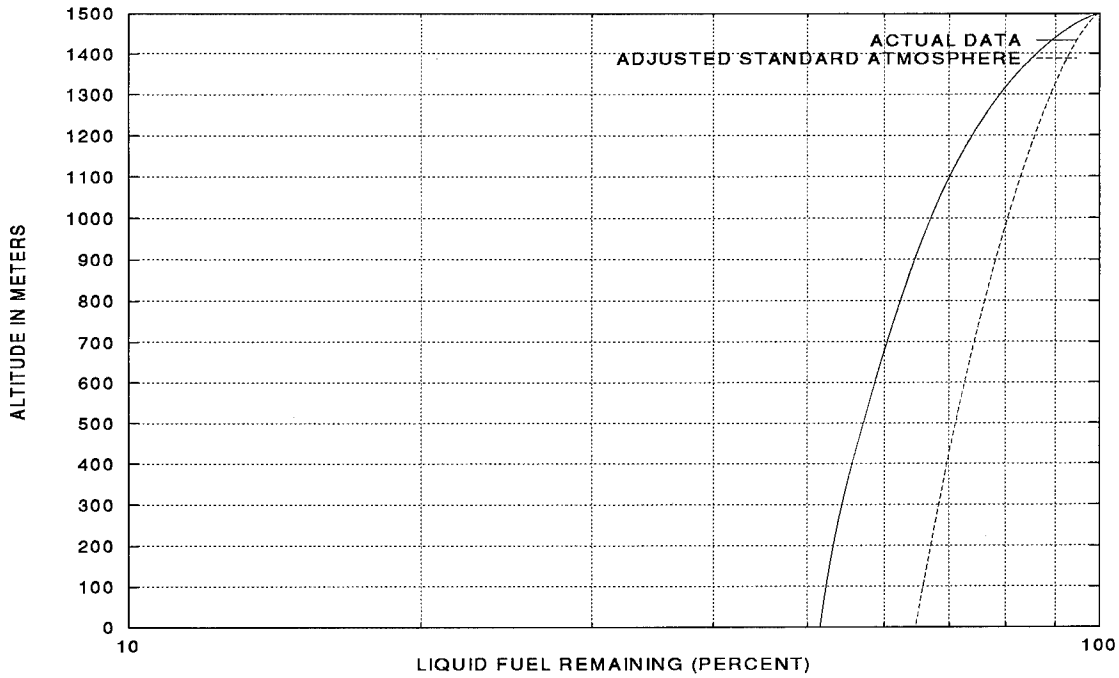

Figure 4.19 Dayton study, DF #2 ground fall

to 10^4 seconds) over which the fuel droplets will continue to advect and disperse. While two case studies are hardly exhaustive, these cases suggest that large errors in predicted ground contamination are possible if no consideration is given to representative meteorology. From our results, however, these errors seem to be conservative, significantly overestimating ground contamination from liquid fuel.

4.7 Sample Calculations from the Integrated Model

4.7.1 Overview. From the results we have presented, we conclude that our model is functioning as designed. We now present sample calculations from the integrated model, following a simulation from release to final ground fall with detailed model output on location and concentration of remaining liquid fuel. For these sample calculations, we use the iterative Fourier method described in Section 3.6.4.2, with the initial data modeled with a Gaussian "ramp-up" along the plume length.

Clewell made several calculations for maximum ground contamination using a simple box model [8:73–75]. Using this model, the maximum ground level contamination was calculated with [8:74]:

$$C = \frac{10PQ}{VW} \tag{4.1}$$

where

C = maximum liquid fuel contamination in mg/s^2

P = percentage of fuel reaching the ground in liquid form

Q = jettison rate in kg/s

V = release airspeed in m/s

W = estimated width of plume in kilometers

This calculation spreads an infinite line source Q/V over the width of the plume W at the time of maximum ground contamination. The scaling factor $10P$ represents the remaining liquid fuel at ground fall. Clewell based his parameterizations on data from evaporation calculations with representative droplet distributions. We assume a monodisperse system such that all droplets make ground fall simultaneously; thus, our time of maximum ground contamination is coincident with time of descent. To account for differences in downwind and crosswind releases, Clewell used two different formulations for the plume width W. For downwind releases,

$$W = 2.4H^2$$

where H is the release height in kilometers. For crosswind releases, this became

$$W = 0.06U(40H^2 - NH)$$

where U is the mean wind speed in meters per second and N is 18, 12 or 10 minutes per kilometer for surface temperatures of 0°C, −20°C, and −40°C respectively [8:74]. We note that because this box model uses an infinite line source, thus there is no time-like variable for duration of release; Equation 4.1 assumes the duration of the release is infinite.

We compare Clewell's results with two calculations performed with the integrated model, a typical KC-135 jettison in Section 4.7.2 and a typical F-111 jettison in Section 4.7.3. Typical values are based on Clewell's summary and analysis of Air Force jettison reports [9, 10]. Comparisons with the Clewell's results demonstrate that our model results are physically meaningful. To demonstrate that our model is numerically sound, we examine our model results compared to an infinite line source calculation in Section 4.7.4.

4.7.2 Case 1: An Example KC-135 Release. We first examined a KC-135 release with the following attributes

- Release airspeed 175 m/s
- Jettison rate 50 kg/s
- Release height 6 kilometers
- Initial plume width 100 meters
- Ground-level temperature -20°C
- Wind from 270° at 4 m/s

We assumed a duration of 5 minutes, typical for the KC-135 based on Air Force fuel jettison reports [9, 10]. Consistent with Clewell, we examined both downwind

(parallel to the mean wind) releases and crosswind (perpindicular to the mean wind) releases. For reference, we started the jettison over Dayton, Ohio, at latitude 39.54 (North) and longitude -84.12 (West). Results are summarized and compared to the box model calculations in Table 4.3.

For the downwind release, the aircraft heading was taken as 270°, while for the crosswind release the aircraft heading was taken as 180°. Figures 4.20 and 4.21 show the map-relative results for the downwind and crosswind release for Case 1. We expect the downwind release to maintain its line source character at ground fall because of the preferential dispersion along the plume length. Similarly, we expect the crosswind release to look like an area source because of preferential dispersion along the plume width. At first glance, Figures 4.20 and 4.21 do not appear to follow our intuition. We explain this by noting that the latitude and longitude scales differ relative to each other to improve the readability of the contour plot. Further, we observe that [26:35–36]:

$$\begin{aligned} 1^\circ \text{ latitude} &\approx 111 \text{ kilometers} \\ 1^\circ \text{ longitude} &\approx 111 \text{ km } \cos(\text{latitude}) \end{aligned}$$

Even if we scaled both axes in Figures 4.20 and 4.21 to reflect the same width in degrees we would observe some distortion of the figure. Grid-relative output for Case 1 is shown in Figures 4.22 and 4.23 using a fixed scale; hence the appearance of these plots is more in line with our intuition.

We observe that our predicted maximum concentrations (extracted from the gridded model output) are about an order of magnitude larger than Clewell's box model predictions. This appears to be an interesting result, since we might expect the box model calculation to be more conservative than our calculations. To explain this difference, we examine y-axis (plume width) cross sections in Figures 4.24 and 4.25. These cross sections depict not only the peak concentration in each model prediction but also the mass contained in each prediction. The box model prediction has been

Downwind	Clewell	Current
Contamination (kg/m^2)	$2.7 \cdot 10^{-7}$	$6.8 \cdot 10^{-6}$
Plume width (km)	90	0.9
Mass in y-axis ($kg^{1/2}$)	0.155	0.146
Crosswind	Clewell	Current
Contamination (kg/m^2)	$7.0 \cdot 10^{-8}$	$2.1 \cdot 10^{-6}$
Plume width (km)	330	2.6
Mass in y-axis ($kg^{1/2}$)	0.152	0.146

Table 4.3 Comparison of results for Case 1

deliberately centered approximately on the dispersion model output. Although we predict a higher maximum concentration, we claim that the box model calculation is dispersing the same amount of mass in a less conservative manner. To support our assertion, we modified our model to calculate and report the y-axis mass (in units of $kg^{1/2}$) at the end of the model calculation. To compute a similar quantity using the box model results, we consider a 1 meter wide strip across the plume, using the calculated plume width to derive an area. We multiply this area by the predicted concentration to arrive at a mass, then take the square root of this mass to arrive at our parameter for comparison. Examining these entries in Table 4.3, we observe very close agreement between the dispersion model y-axis mass and the box model y-axis mass. We conclude that our results are physically meaningful and are indeed similar to Clewell's box model predictions; our detailed dispersion calculation, however, yields a significant improvement in assessing the largest point contamination areas (i.e. along the center line).

In Equation 4.1, plume width refers to the physical dimension of the single maximum concentration isopleth at the ground. In order to compare our model calculations with Clewell's results, we used a similar measure for the width of maximum concentration at the ground. The width of maximum concentration is calculated as the distance across the plume within which all concentration values greater than or equal to 95% of the maximum (centerline) concentration fall.

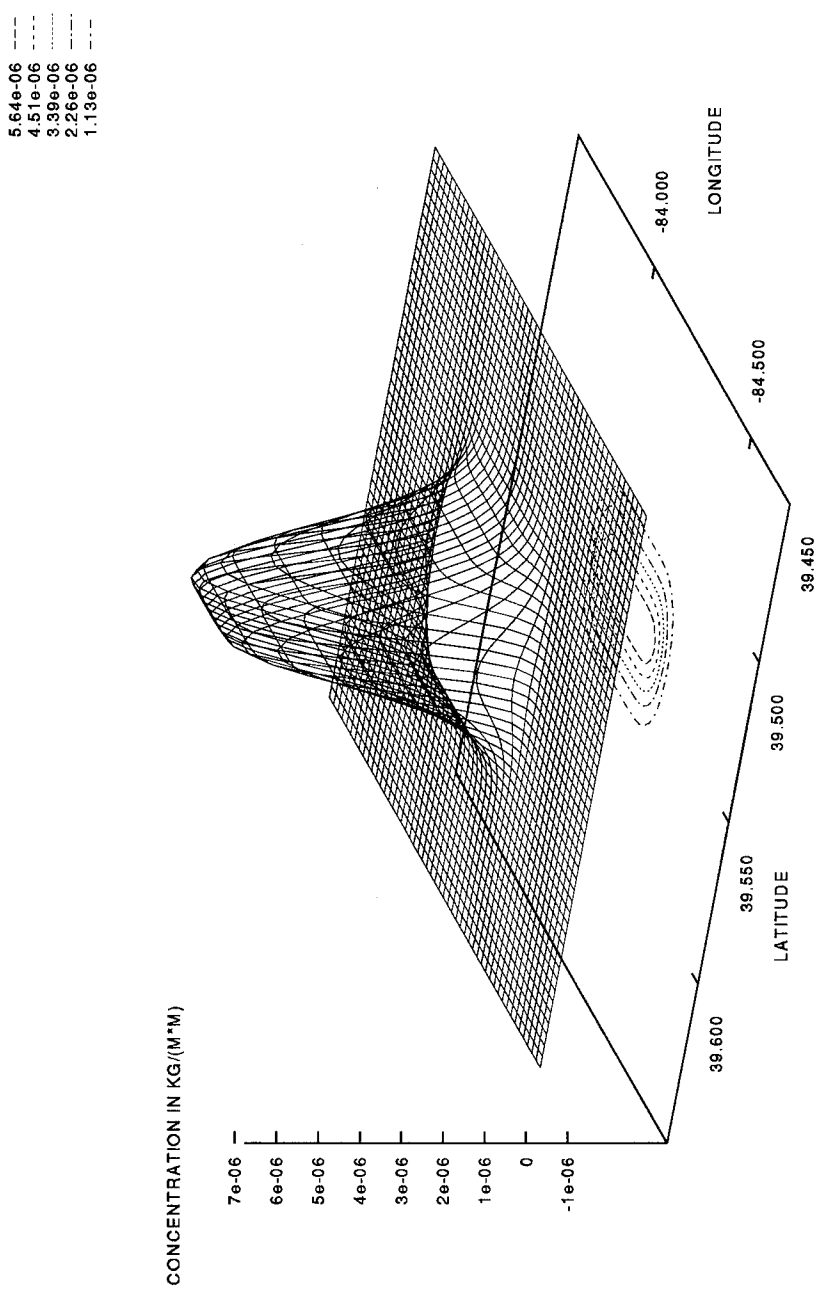

Figure 4.20 Map-relative output for Case 1, downwind release

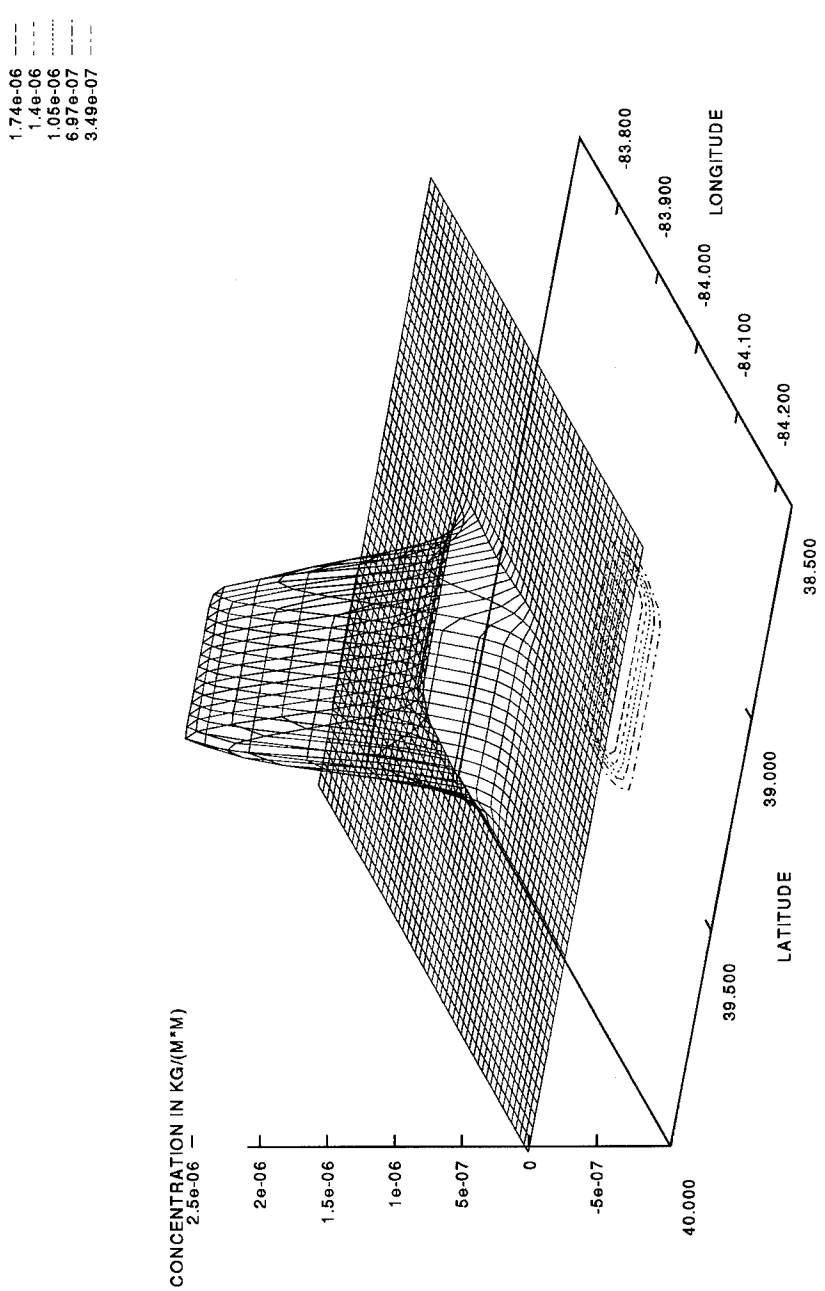

Figure 4.21 Map-relative output for Case 1, crosswind release

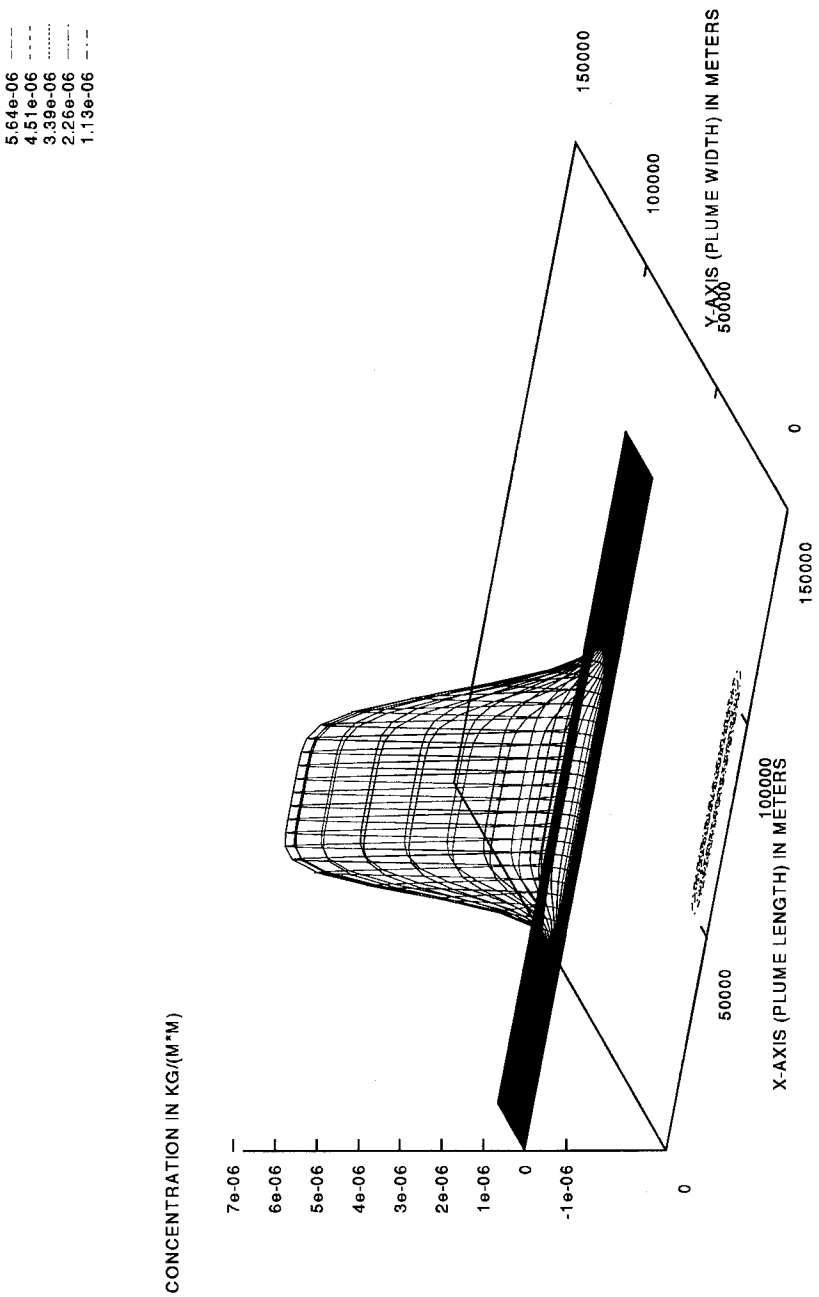

Figure 4.22 Grid-relative output for Case 1, downwind release

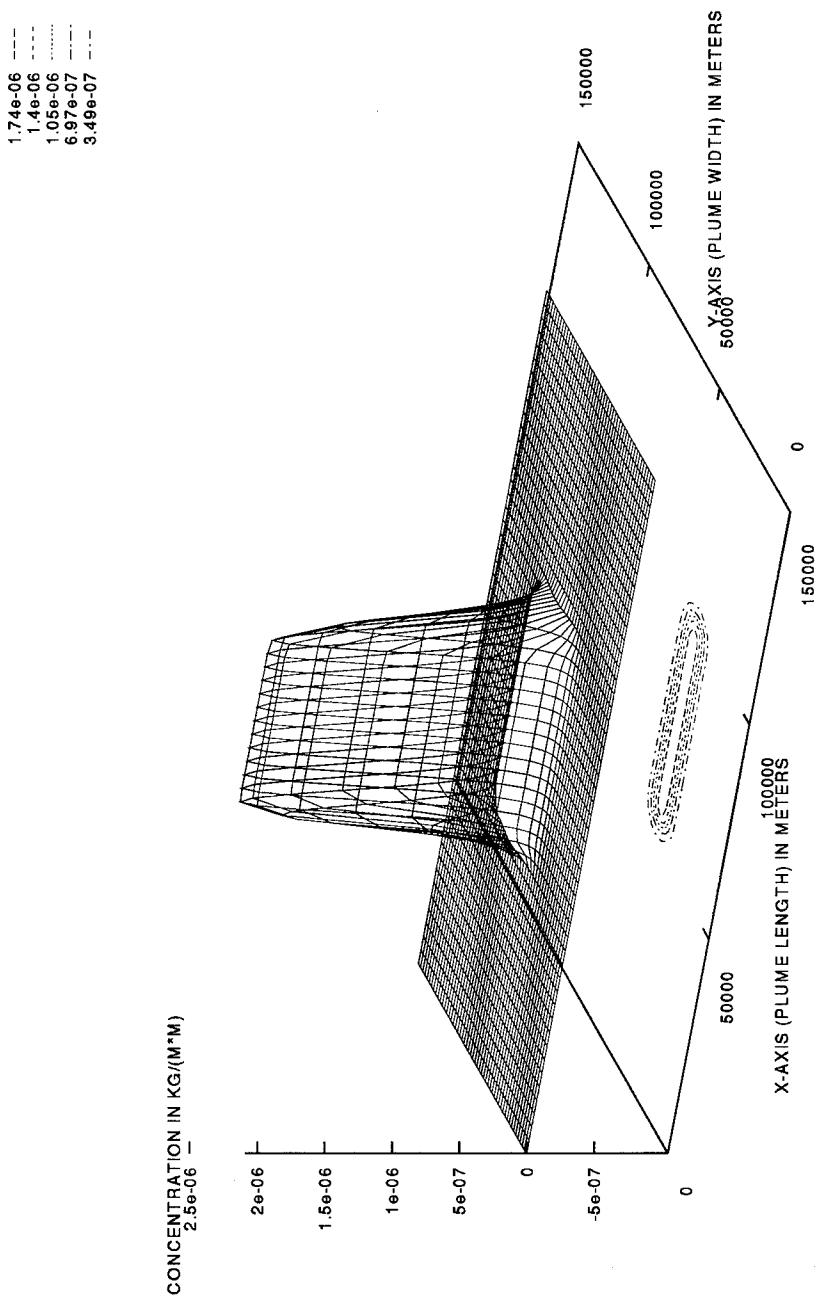

Figure 4.23 Grid-relative output for Case 1, crosswind release

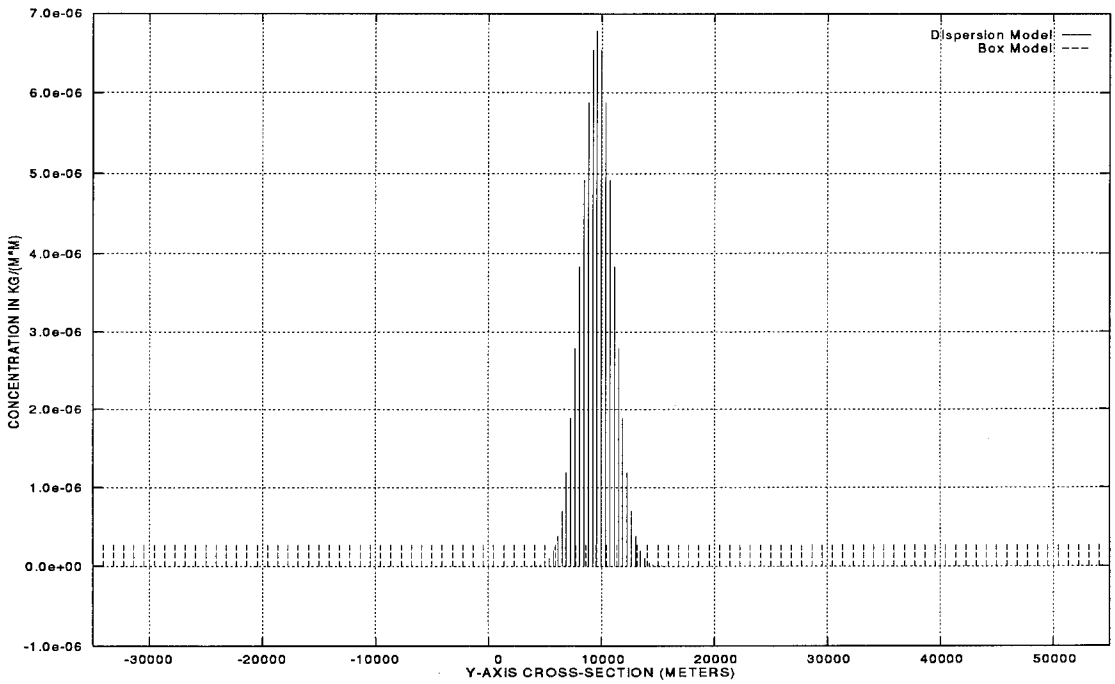

Figure 4.24 Cross-section of the plume width for Case 1, downwind release

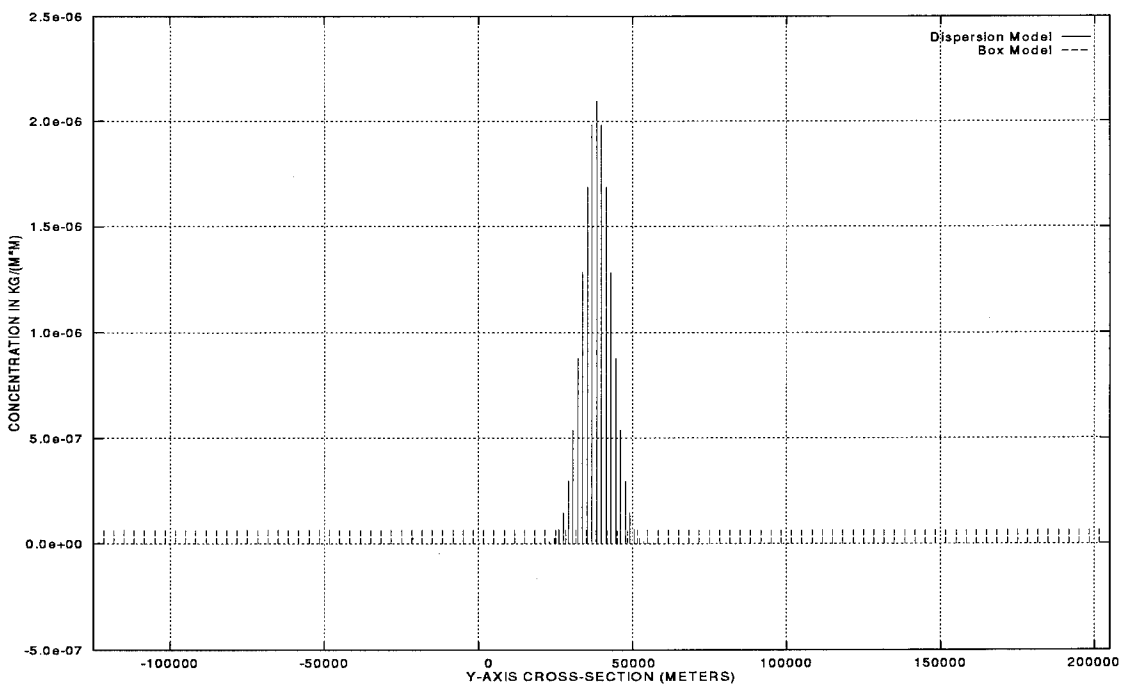

Figure 4.25 Cross-section of the plume width for Case 1, crosswind release

4.7.3 Case 2: An Example F-111 Release. We examined an F-111 jettison with the following attributes

- Release airspeed 175 m/s
- Jettison rate 17 kg/s
- Release height 1.5 kilometers
- Initial plume width 20 meters
- Ground-level temperature 0°C
- Wind from 270° at 5 m/s

We assumed a duration of 2 minutes, again consistent with Clewell's earlier work [9, 10]. As in Case 1, we examine both downwind and crosswind releases with headings of 270° and 180° respectively.

Map-relative results are depicted in Figures 4.26 and 4.27, with fixed-scale, grid-relative plots in Figures 4.28 and 4.29. Qualitatively, these contour plots appear similar to Case 1; that is, the downwind release maintains a line source character, while the crosswind release evolves into an area source.

Results are summarized in Table 4.4. As in Case 1, we predict higher peak concentrations than those predicted by the box model. Cross sections in Figures 4.30 and 4.31 show, however, that our model calculations and the box model calculations are dispersing the same mass (see Table 4.4). For Case 2 our predictions are two to three times larger than the box model predictions vice the 25 to 30 times larger predictions for Case 1. We suspect that we have a closer agreement with the box model because our distribution at the ground is more box-like (i.e. the edges of the plume are sharper) than Case 1. We note that the Case 1 descent is 173 minutes, while the Case 2 descent is 132 minutes; thus, Case 1 has a longer time to disperse. Further, Case 2 has a higher wind speed (5 m/s vice 4 m/s) which results in a smaller $\Delta\theta$ (628 m^2/s vice 1048 m^2/s) in the direction of the wind. We conclude, as in Case 1, that we are generating physically meaningful results.

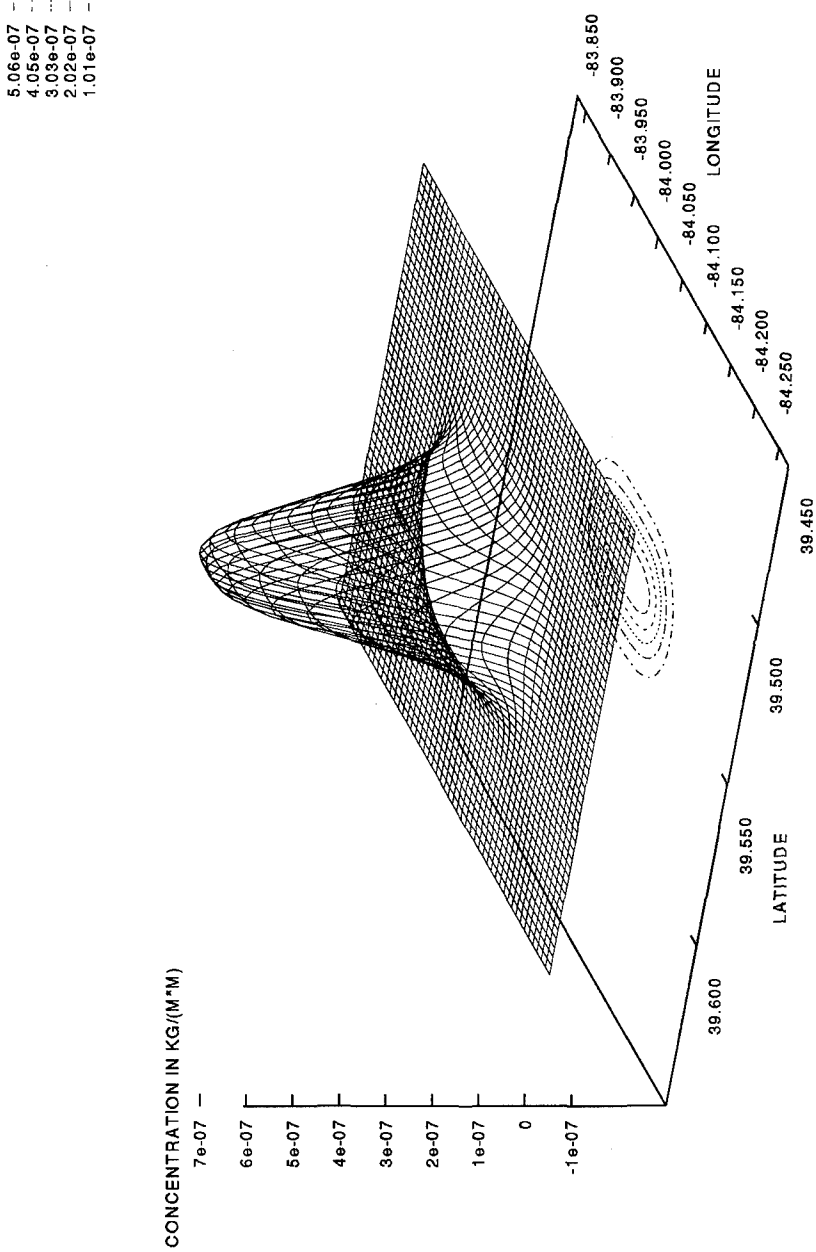

Figure 4.26 Map-relative output for Case 2, downwind release

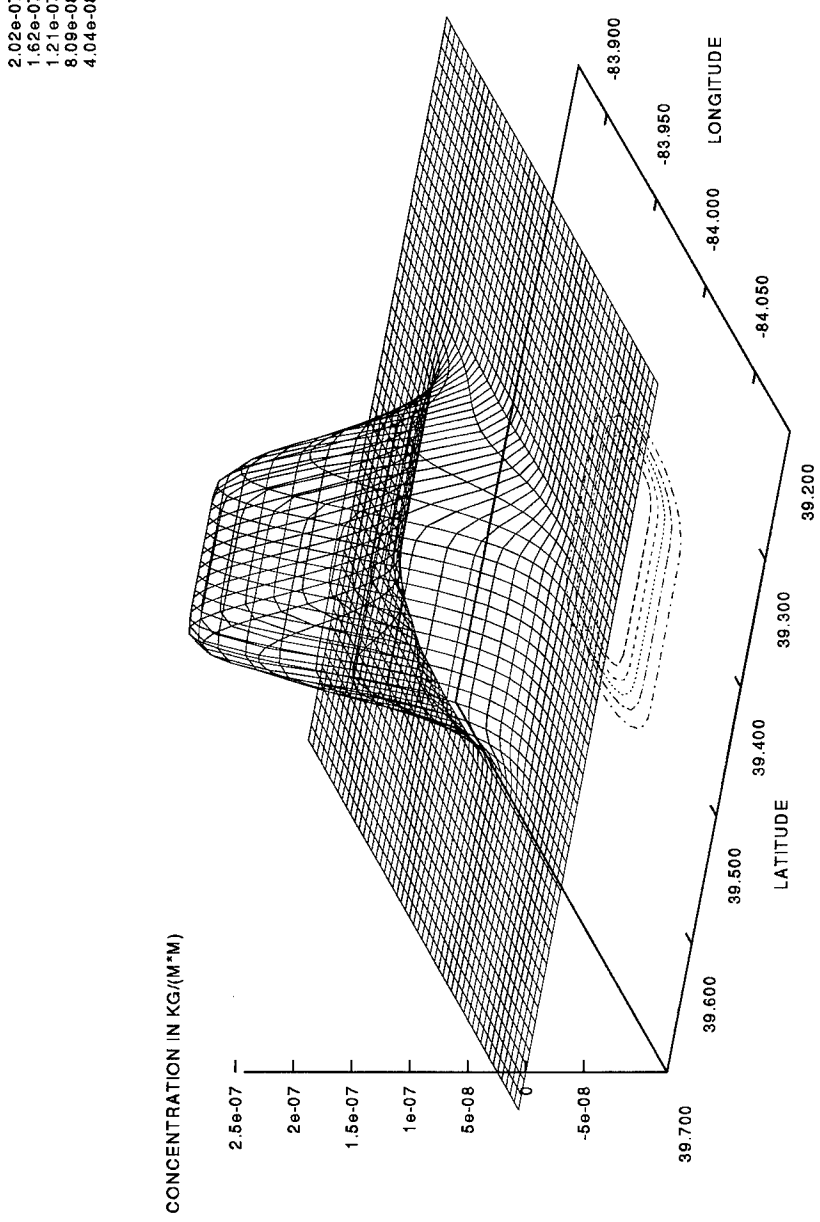

Figure 4.27 Map-relative output for Case 2, crosswind release

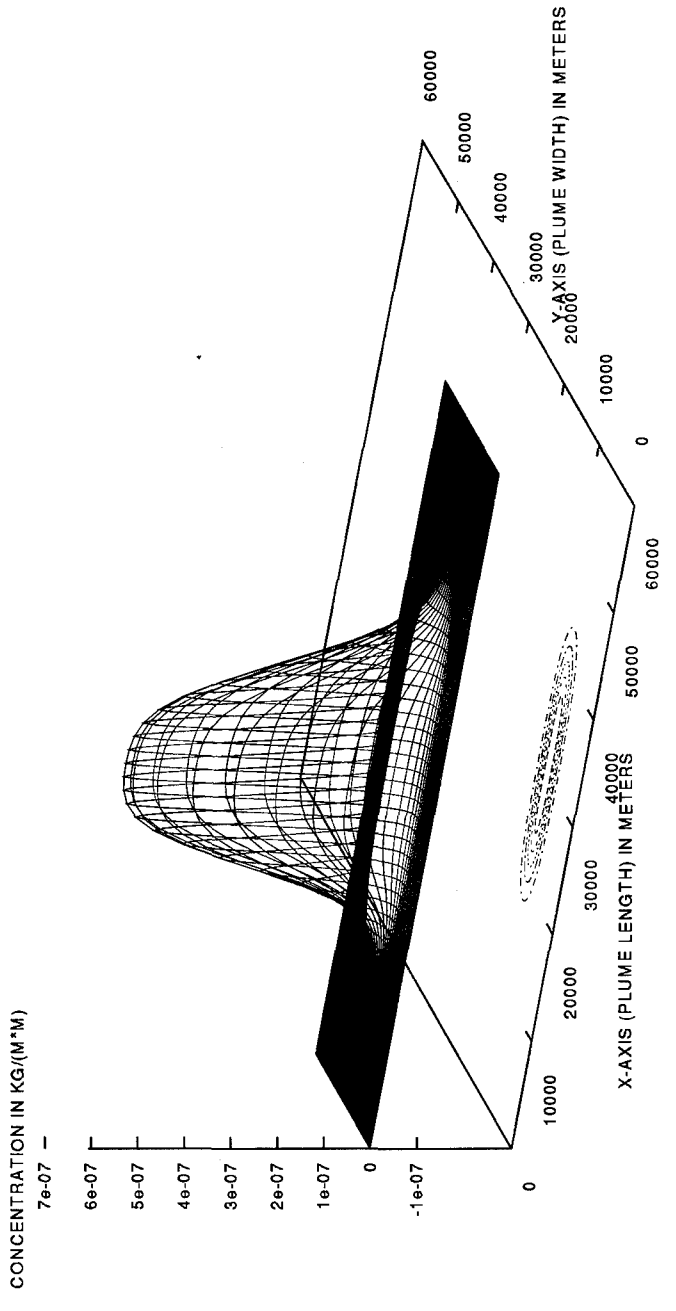

Figure 4.28 Grid-relative output for Case 2, downwind release

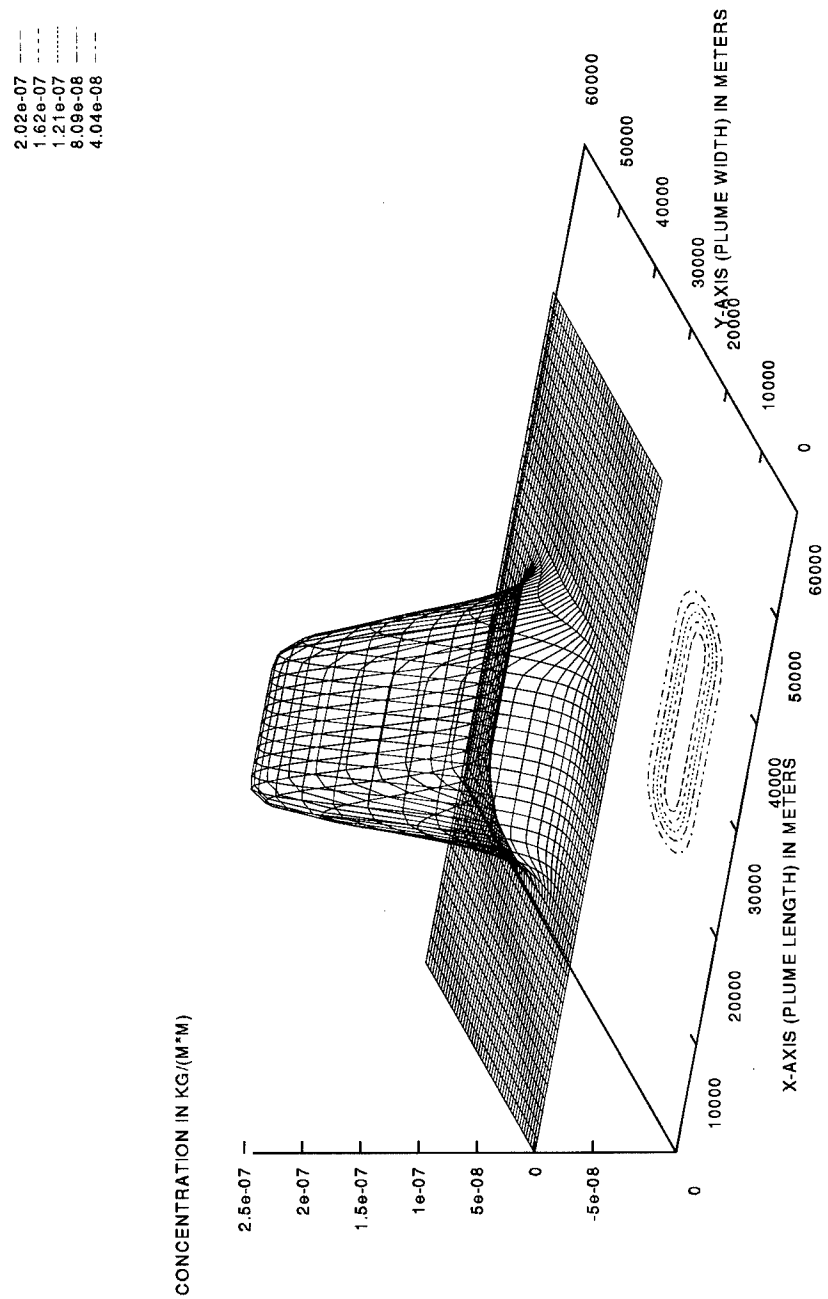

Figure 4.29 Grid-relative output for Case 2, crosswind release

Downwind	Clewell	Current
Contamination (kg/m^2)	$2.8 \cdot 10^{-7}$	$6.1 \cdot 10^{-7}$
Plume width (km)	5	0.7
Mass in y-axis (kg$^{1/2}$)	0.037	0.041
Crosswind	Clewell	Current
Contamination (kg/m^2)	$8.0 \cdot 10^{-8}$	$2.4 \cdot 10^{-7}$
Plume width (km)	19	1.8
Mass in y-axis (kg$^{1/2}$)	0.039	0.041

Table 4.4 Comparison of results for Case 2

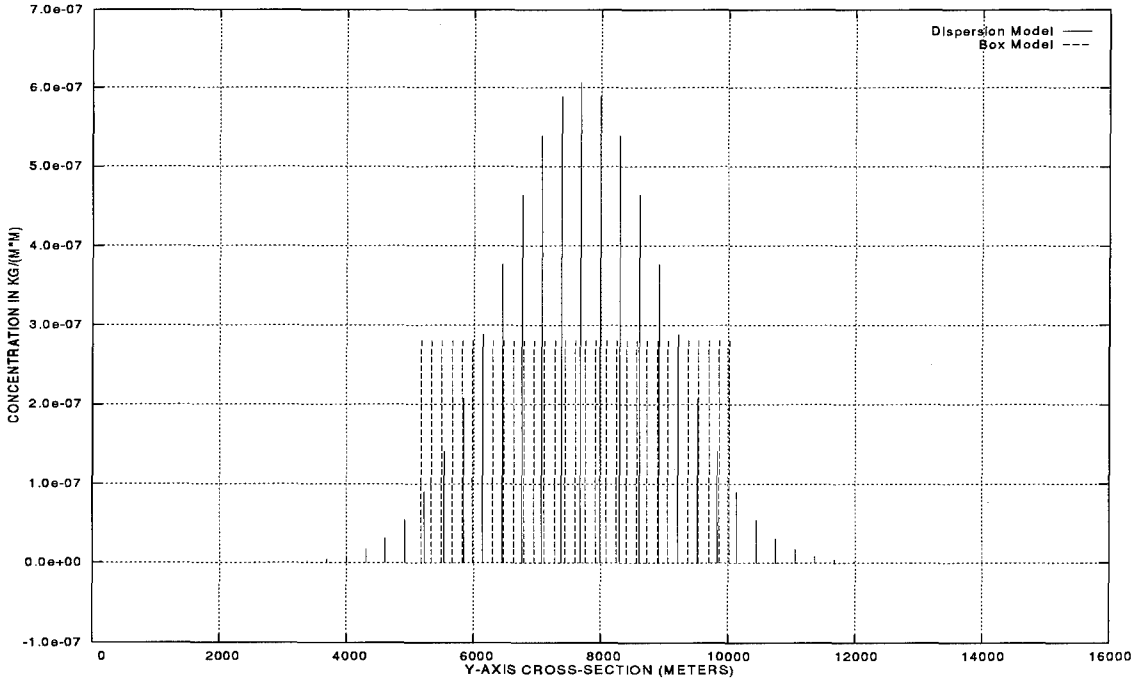

Figure 4.30 Cross-section of the plume width for Case 2, downwind release

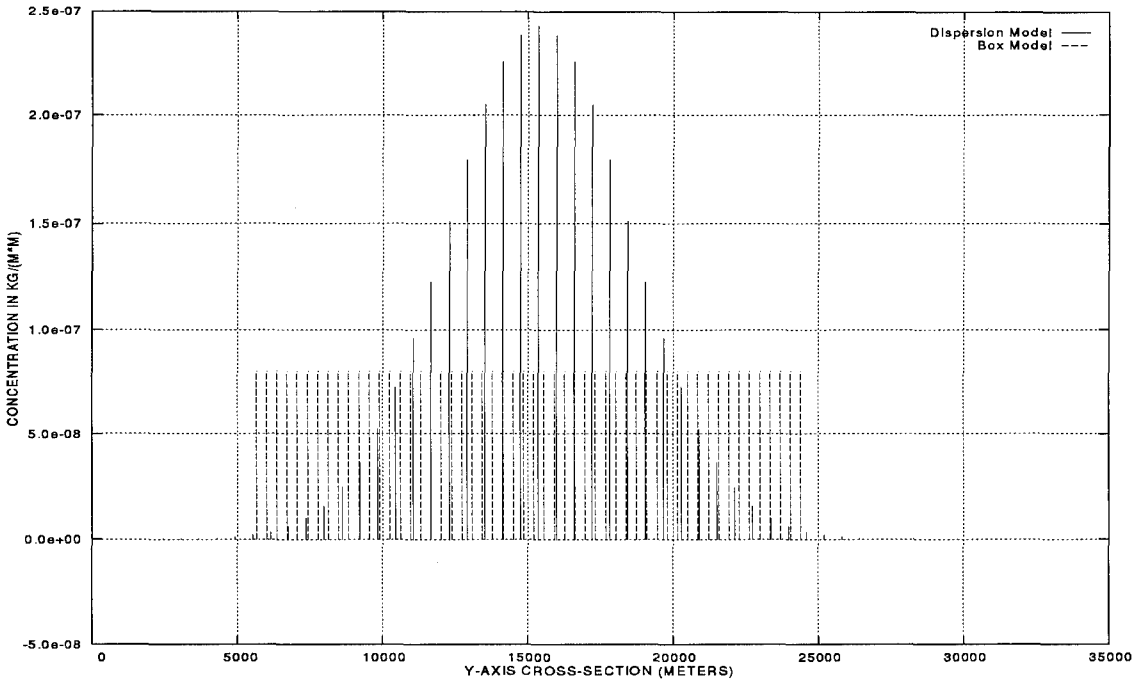

Figure 4.31 Cross-section of the plume width for Case 2, crosswind release

4.7.4 An Infinite Line Source Calculation. To provide further verification of our results, we derive an infinite line source calculation. We begin with the three-dimensional diffusion equation [27:535]

$$\frac{\partial c}{\partial t} = K_x \frac{\partial^2 c}{\partial x^2} + K_y \frac{\partial^2 c}{\partial y^2} + K_z \frac{\partial^2 c}{\partial z^2} \tag{4.2}$$

For an instantaneous point source at (x_0, y_0, z_0), with constant diffusivity parameters and source strength Q, this has the analytic solution ([15:51]

$$c(x,y,z,t) = \frac{Q}{(4\pi t)^{3/2}(K_x K_y K_z)^{1/2}} \exp\left[-\frac{(x-x_0)^2}{4K_x t} - \frac{(y-y_0)^2}{4K_y t} - \frac{(z-z_0)^2}{4K_z t}\right] \tag{4.3}$$

To derive an analytic solution for a line source coincident with the x-axis, we take Q^* to be the line source strength and integrate Equation 4.2 thus:

$$\begin{aligned} c(y,z,t) &= \int_{-\infty}^{\infty} \frac{Q^*}{(4\pi t)^{3/2}(K_xK_yK_z)^{1/2}} \exp\left[-\frac{(x-x_0)^2}{4K_xt} - \frac{(y-y_0)^2}{4K_yt} - \frac{(z-z_0)^2}{4K_zt}\right] dx \\ &= \frac{Q^*}{4\pi t(K_yK_z)^{1/2}} \exp\left[-\frac{(y-y_0)^2}{4K_yt} - \frac{(z-z_0)^2}{4K_zt}\right] \end{aligned} \tag{4.4}$$

which is similar to a form of the line source equation presented in Lowell [21:7]. We assume that all the material in the vertical column over a point in the xy-plane strikes the ground simultaneously. To reflect this in our line source calculation, we integrate along the z-axis from $-\infty$ to ∞ thus:

$$c(y,t) = \int_{-\infty}^{\infty} \frac{Q^*}{4\pi t(K_yK_z)^{1/2}} \exp\left[-\frac{(y-y_0)^2}{4K_yt} - \frac{(z-z_0)^2}{4K_zt}\right] dz \tag{4.5}$$

To complete this integration, we make the substitution $a = (4K_zt)^{-1/2}$ and use the fact that

$$\int_{-\infty}^{\infty} e^{-a^2x^2} dx = \frac{1}{a}\sqrt{\pi}$$

to arrive at

$$c(y,t) = \frac{Q^*}{2(\pi K_yt)^{1/2}} \exp\left(-\frac{(y-y_0)^2}{4K_yt}\right) \tag{4.6}$$

We note that if Q has dimension of mass per unit length, our expression for $c(y,t)$ has dimension of mass per unit area, consistent with our model calculations. If we consider only the maximum concentration in the context of Equation 4.6, this maximum is necessarily on the center line, at $y = y_0$, so that

$$c(t) = \frac{Q^*}{2(\pi K_yt)^{1/2}} \tag{4.7}$$

Using this equation as an estimator for maximum concentration, we revisit our model results for the KC-135 release and the F-111 short-duration (Case 2) release. Results are summarized in Table 4.5.

We consider the original line source strength at release Q^* and multiply this number by the mass fraction remaining at ground fall. The form of Equation 4.7 is such that at $t = 0$, $c(t)$ is infinite. Clearly our model does not start with these initial conditions; we always assume a finite initial concentration distribution. For Case 1, our initial maximum centerline concentration is $c_0 = 4.27 \cdot 10^{-3}$ kg/m^2. For Case 2, our initial maximum centerline concentration is $c_0 = 7.26 \cdot 10^{-3}$ kg/m^2. We rearrange Equation 4.7 to calculate the time at which our model initial condition c_0 is valid:

$$t = \frac{1}{4\pi K_y} \left(\frac{Q^*}{c_0} \right)^2 \tag{4.8}$$

The largest value for t in the cases considered is for the crosswind release in Case 1, resulting in $t = 3$ seconds. The time scale Θ of these cases is on the order of 10^3 to 10^4 seconds (see Table 4.5). We assume, then, that the theoretical line source quickly evolves into the area source we use as an initial condition for the model. Thus, the times used in Table 4.5 are the times of descent of the droplets.

We observe from Table 4.5 that our model results show close agreement with the infinite line source calculation. From this agreement we conclude that our model is numerically sound. We note that this infinite line source calculation uses the same K_y derived in Section 3.6.5. Thus, we do not claim that these results reinforce the physical character of our model; both calculations (dispersion model and infinite line source) are only as good as the diffusion coefficients. We do note that the iterative Fourier solution and the derived line source calculation (Equation 4.6) solve exactly the same differential equation and should have very nearly the same solution for $t > 3$ seconds near the center of the plume (where we are examining the maximum concentrations). That we do not see extremely close agreement in Table 4.5 is probably due to the initial conditions for the iterative Fourier technique not exactly matching the distribution of the "evolved" line source at $t = 3$. That is, the initial conditions we assume for the jettisoned plume do not assume a history as a strict line source with infinite concentration at $t = 0$.

	Q^* (kg/m)	Fraction	K_y (m^2/s)	t (seconds)	Model Results	Line Source
Case 1						
Downwind	0.286	0.078	100	10368	$6.8 \cdot 10^{-6}$	$6.2 \cdot 10^{-6}$
Crosswind	0.286	0.078	1048	10368	$2.1 \cdot 10^{-6}$	$1.9 \cdot 10^{-6}$
Case 2						
Downwind	0.092	0.018	100	7920	$6.1 \cdot 10^{-7}$	$5.2 \cdot 10^{-7}$
Crosswind	0.092	0.018	628	7920	$2.4 \cdot 10^{-7}$	$2.1 \cdot 10^{-7}$

Table 4.5 Comparison of model results with line source calculation

Given that this infinite line source calculation appears to be in good agreement with our model results, we might ask: why not use the line source calculation? Our sample calculations are necessarily simple cases, with constant wind profiles and hence constant diffusion coefficients. More realistic problems using actual meteorological observations could not be treated so simply. Further, we cannot get a good sense of the complete plume dimension with the infinite line source; by assumption the length along the release path is infinite. The computational complexity introduced in our model is necessary, then, to calculate complete information about ground contamination.

4.7.5 Conclusions. Overall, we found good agreement between maximum concentration results from our model calculations and from Clewell's box model. From these results we conclude our model is physically sound. Additional comparisons with an infinite line source calculation show that our method is numerically sound.

4.8 Summary

Our goal in this research was to develop a general tool for predicting the fate of jettisoned aviation fuel. We have presented results to demonstrate the soundness of our design and implementation, and sample calculations to demonstrate model output. Our calculations are producing physically meaningful results, though we have neither exhaustively studied the model behaviour nor attempted to calibrate

some of the model parameterizations (e.g. the eddy diffusion parameters). We now offer a summary of our research, with recommendations for further efforts.

V. Summary and Conclusions

5.1 Summary

Aircraft in flight must occasionally jettison unburned aviation fuel into the atmosphere. A body of literature exists to determine how much of this unburned fuel may contaminate the ground; however, little work has been accomplished to determine the transport and dispersion of this material. We have presented our answer to the question: *Where and in what concentration will jettisoned aviation fuel make ground fall?*. Our presentation has focused on generalizing this query into a tool for assessing the threat of ground contamination from any aviation fuel in a wide variety of fuel jettison scenarios.

5.2 Conclusions

We have successfully designed and implemented an evaporation, advection and dispersion model capable of predicting ground fall location and concentration of an aviation fuel following a fuel jettison event. We have demonstrated that our calculations produce physically meaningful results, in reasonable agreement with previously published work. In designing our model, we have improved previous work in droplet evaporation by incorporating near real-time meteorological information. In brief case studies, we have demonstrated that this data can significantly improve model predictions.

5.3 Recommendations

While we have verified that model calculations are correct, we have only briefly touched on the investigations possible with our general tool.

We have shown that meteorological conditions are potentially significant in the evaporation (and consequently the advection and dispersion) of jettisoned fuel. Given the availability of weather data over the internet and through other public

sources, many location-specific and climate-specific studies are possible. These kinds of studies may be useful in assessing long-term effects of repeated fuel jettisoning in a geographic region.

We have limited our studies to the aviation fuels JP-4 and JP-8, using DF #2 as an upper bound on low-evaporation fuels. The model is capable of using any aviation fuel, however. Other fuels, especially newer or broadened-specification fuels, would make useful studies, both to improve knowledge about potential ground contamination and to improve knowledge about the model.

The eddy diffusion parameters within the model are currently based on order-of-magnitude estimates using wind speed and wind variation. We have noted that these parameterizations appear to overestimate diffusion along the axis of the mean wind. Significant improvement to the model physics could be made with a study and calibration of these coefficients.

We have mentioned that little previous work exists on the dispersion of jettisoned fuel. We should note, though, that line source models for air pollution transport are available from the Environmental Protection Agency (EPA), among other sources. Studies using our model in conjunction with an air pollution line source model would significantly improve knowledge about the model developed in this research.

Appendix A. Clewell's Fuel Component Models

In generating and comparing our model results with previous work, we use the multi-component fuel models developed by Clewell for his ground contamination studies. Tables A.1, A.2, and A.3 are physically identical to the original models published in Clewell [11:5–7], though we have accomplished unit conversions for ease of use in model calculations.

Component	Volume Fraction	Molecular Weight	Boiling Point (K)	Density at 20°C (kg/m^3)
C5 hydrocarbons	0.039	72.2	301.1	620.0
C6 paraffins	0.081	86.2	333.4	660.0
C6 cycloparaffins	0.021	84.2	353.9	780.0
Benzene	0.003	78.1	353.2	880.0
C7 paraffins	0.094	100.2	364.9	690.0
C7 cycloparaffins	0.071	98.2	374.1	770.0
Toluene	0.007	92.1	383.9	870.0
C8 paraffins	0.101	114.2	390.9	700.0
C8 cycloparaffins	0.074	112.2	397.4	780.0
C8 aromatics	0.016	106.2	412.2	870.0
C9 paraffins	0.091	128.3	415.6	720.0
C9 cycloparaffins	0.043	126.2	427.6	800.0
C9 aromatics	0.024	120.2	438.4	880.0
C10 paraffins	0.073	142.3	432.8	720.0
C10 cycloparaffins	0.037	140.3	444.1	800.0
C10 aromatics	0.018	134.2	450.2	860.0
Napthalene	0.002	128.2	491.1	1030.0
C11 paraffins	0.048	156.3	469.1	740.0
C11 cycloparaffins	0.025	154.3	469.6	800.0
Dicycloparaffins	0.034	150.3	474.1	890.0
C11 aromatics	0.011	148.2	478.1	860.0
C11 napthalenes	0.002	142.2	517.8	1020.0
C12 paraffins	0.028	170.3	489.4	750.0
C12 cycloparaffins	0.012	168.3	484.1	800.0
C12 aromatics	0.005	162.3	489.1	860.0
C12 napthalenes	0.002	156.2	541.1	1000.0
C13 paraffins	0.011	184.4	508.6	760.0
C13 cycloparaffins	0.004	182.4	498.1	800.0
C13 aromatics	0.001	176.3	507.1	870.0
C14 hydrocarbons	0.002	198.4	526.9	760.0
C15 hydrocarbons	0.001	212.4	543.8	770.0
Tricycloparaffins	0.018	192.4	563.1	940.0
Residual hydrocarbons	0.001	202.3	666.1	1270.0

Table A.1 Clewell's 33-component model for JP-4 [11:5]

Component	Volume Fraction	Molecular Weight	Boiling Point (K)	Density at 20°C (kg/m^3)
C8 paraffins	0.003	114.2	391.1	700.0
C8 cycloparaffins	0.002	112.2	397.1	780.0
C8 aromatics	0.001	106.2	412.1	870.0
C9 paraffins	0.024	128.3	415.1	720.0
C9 cycoloparaffins	0.015	126.2	427.1	800.0
C9 aromatics	0.010	120.2	438.1	880.0
C10 paraffins	0.056	142.3	433.1	720.0
C10 cycloparaffins	0.035	140.3	444.1	800.0
C10 aromatics	0.023	134.2	450.1	860.0
C11 paraffins	0.087	156.3	469.1	740.0
C11 cycloparaffins	0.033	154.3	469.1	800.0
Dicycloparaffins	0.031	152.3	474.1	890.0
C11 aromatics	0.036	148.2	478.1	860.0
C12 paraffins	0.108	170.3	489.1	750.0
C12 cycloparaffins	0.080	166.3	494.1	880.0
C12 aromatics	0.046	162.3	489.1	860.0
C13 paraffins	0.115	184.4	508.1	760.0
C13 cycloparaffins	0.085	182.4	498.1	800.0
C13 aromatics	0.049	176.3	507.1	870.0
C14 paraffins	0.059	198.4	527.1	760.0
C14 cycloparaffins	0.044	192.4	563.1	940.0
C14 aromatics	0.025	186.3	568.1	1030.0
C15 paraffins	0.014	212.4	544.1	770.0
C15 cycloparaffins	0.010	206.4	573.1	900.0
C15 aromatics	0.006	200.4	578.1	950.0
C16 hydrocarbons	0.002	226.4	560.1	770.0
Residual hydrocarbons	0.001	202.3	666.1	1270.0

Table A.2 Clewell's 27-component model for JP-8 [11:6]

Component	Volume Fraction	Molecular Weight	Boiling Point (K)	Density at 20°C (kg/m^3)
C10 paraffins	0.009	142.3	433.1	720.0
C10 cycloparaffins	0.006	140.3	444.1	800.0
C10 aromatics	0.004	134.2	450.1	860.0
C11 paraffins	0.023	156.3	469.1	740.0
C11 cycloparaffins	0.017	152.3	474.1	890.0
C11 aromatics	0.010	148.2	478.1	860.0
C12 paraffins	0.038	170.3	489.1	750.0
C12 cycloparaffins	0.028	166.3	494.1	880.0
C12 aromatics	0.016	162.3	489.1	860.0
C13 paraffins	0.064	184.4	508.1	760.0
C13 cycloparaffins	0.048	182.4	498.1	800.0
C13 aromatics	0.028	176.3	507.1	870.0
C14 paraffins	0.088	198.4	527.1	760.0
C14 cycloparaffins	0.066	192.4	563.1	940.0
C14 aromatics	0.038	186.3	568.1	1030.0
C15 paraffins	0.074	212.4	544.1	770.0
C15 cycloparaffins	0.055	206.4	573.1	900.0
C15 aromatics	0.032	200.4	578.1	950.0
C16 paraffins	0.058	226.4	560.1	770.0
C16 cycloparaffins	0.044	222.4	568.1	880.0
C16 aromatics	0.025	214.4	598.1	950.0
C17 paraffins	0.055	240.5	576.1	780.0
C17 cycloparaffins	0.041	236.5	583.1	880.0
C17 aromatics	0.024	232.5	578.1	890.0
C18 paraffins	0.043	254.5	579.1	780.0
C18 cycloparaffins	0.032	248.5	608.1	900.0
C18 aromatics	0.018	242.5	613.1	1000.0
C19 paraffins	0.007	268.5	603.1	780.0
C19 cycloparaffins	0.006	262.6	633.1	900.0
C19 aromatics	0.003	244.5	673.1	1200.0

Table A.3 Clewell's 30-component model for DF #2 [11:7]

Appendix B. A User's Guide to the Fuel Jettison Simulation

B.1 Running the Model

We present essential information for running the integerated evaporation, advection and dispersion model. The model executable is called **model**, and is invoked with

model *model.ini*

where *model.ini* is a data file containing the initialization data. Actually, *model.ini* is a file containing a list of file names. Section B.2 lists an example *model.ini* file. Lines beginning with a pound sign (#) are comments and are ignored by the parsing routine. Certain fields are mandatory in the *model.ini* file, but the order of the fields within the file is not important.

The jettison data file contains information related to the release of the fuel (e.g. airspeed, heading, position). A sample jettison data file appears in Section B.3.

The environmental data file contains the upper air data near the jettison event. A sample environmental data file appears in Section B.4.

The fuel data file contains the data about the jettisoned fuel, similar to the information in Appendix A. Section B.5 shows a sample fuel data file.

The message output file is created with the file name specified, or with the default name 'messages.tmp' if no name is specified. Evaporation and advection model output may be directed to this file to trace the progress of the model run.

The grid data output file receives the grid-relative output at the end of the model run, while the map output file receives the map-relative data. These data are separated for ease of plotting.

A complete code listing is available in electronic format via anonymous ftp to

archive.afit.af.mil

in the file

/pub/kpfeiffe/model.zip

B.2 Sample model.ini *File*

```
################################################################################
#
#  file:  model.ini
#
#  DESCRIPTION
#  -----------
#  This is the initialization file for the model.  The name model.ini
#  is arbitrary; this file name is supplied to the model executable
#  on the command line.
#
#  Mandatory fields are:
#
#  jettison_data= (the jettison data file name)
#  environmental_data= (the environmental data file name)
#  fuel_data= (the fuel data file name)
#
#  Optional but recommended fields are:
#
#  output_messages= (message and model output file)
#  output_grid= (grid data output file)
#  output_map= (map data output file)
#
#  If the optional fields are not specified, default file names
#  are assigned to these files.  The message file is intended for
#  tracing information (e.g. What are Kx and Ky at each iteration?)
#  and warning messages.  Critical error messages are always
#  directed to the console
#
jettison_data=kc135.dat
environmental_data=dayton.atm
fuel_data=jp4.dat
output_messages=kc135.msg
output_grid=kc135.grid
output_map=kc135.map
```

B.3 Sample Jettison Data File

```
################################################################################
#
#  file:  case1.dat
#
#  DESCRIPTION
#  -----------
#  This is a jettison data file for the model.
#
#  Valid fields are:
#
#  altitude= (release altitude in meters)
#  airspeed= (airspeed at release in m/s)
#  duration= (duration of release in seconds)
#  heading= (aircraft heading at release)
#  latitude= (aircraft latitude at start of release)
#  longitude= (aircraft longitude at start of release)
#  plume_width= (initial plume width in meters)
#  rate= (jettison rate in kg/s)
#
#  All fields are optional.  If not specified, a field will be
#  assigned a default value.  For latitude and longitude, North
#  and East are positive, and the numbers should be decimal
#  degrees, not degrees and minutes.
#
################################################################################
altitude=1500.0
airspeed=175.0
duration=600.0
heading=180.0
latitude=39.54
longitude=-84.12
mean_drop_diameter=270.0
plume_width=100.0
rate=50.0
```

B.4 Sample Environmental Data File

```
################################################################################
#
#  file:  dayton.atm
#
#  DESCRIPTION
#  -----------
#  This is a sample environmental data file.
#  Valid fields and formats are
#
#    thermo_data=altitude;pressure;temperature;
#
#      where altitude is in meters, pressure is in millibars (hPa)
#      and temperature is in Celsius
#
#    wind_data=altitude;wind direction;wind speed;
#
#      where altitude is in meters, wind direction is in degrees
#      on the compass, and wind speed is in knots
#
#  Data must be sorted highest to lowest altitude.
################################################################################
thermo_data= 6304.4; 468.0;-14.9;
thermo_data= 5770.0; 500.0;-12.7;
thermo_data= 4840.8; 570.0; -6.1;
thermo_data= 4123.9; 624.0;  0.0;
thermo_data= 3115.0; 700.0;  4.8;
thermo_data= 1500.0; 850.0; 16.2;
thermo_data= 1112.8; 890.0; 19.4;
thermo_data=  774.0; 925.0; 20.6;
thermo_data=  452.7; 947.0; 21.0;
thermo_data=    0.0; 978.0; 14.4;
wind_data= 6096.0;275.0; 44.0;
wind_data= 4876.8;265.0; 40.0;
wind_data= 3352.8;260.0; 29.0;
wind_data= 2133.6;300.0; 28.0;
wind_data= 1500.0;280.0; 36.0;
wind_data= 1219.2;275.0; 36.0;
wind_data=  914.4;265.0; 42.0;
wind_data=  774.0;265.0; 42.0;
wind_data=  609.6;255.0; 44.0;
wind_data=  304.8;210.0;  8.0;
wind_data=    0.0;210.0;  7.0;
```

B.5 Sample Fuel Data File

```
##############################################################################
#
#  file:  jp8.dat
#
#  DESCRIPTION
#  -----------
#  This is a sample fuel data file. Valid fields and formats are
#
#  fuel_type=(character string label for the fuel)
#  number_of_components=(integer number of components)
#  component=label;volume percent;molecular weight;boiling point;density;
#
#    where:  label is a character string (maximum 30 characters)
#       describing the component, volume percent.
# volume percent is the volume fraction of the component.
# molecular weight is in kg/kmol
# boiling point is at standard temperature and pressure,
#   in Kelvin
# density is in kg/m^3
#
#  The 'number_of_components=' MUST appear before any components.
#
##############################################################################
fuel_type=JP-8 (Clewell)
number_of_components=27
component=C8 paraffins;  0.003;114.2;391.15; 700.0
component=C8 cycloparaffins;   0.002;112.2;397.15; 780.0
component=C8 aromatics;  0.001;106.2;412.15; 870.0
component=C9 paraffins;  0.024;128.3;415.15; 720.0
component=C9 cycoloparaffins;  0.015;126.2;427.15; 800.0
component=C9 aromatics;  0.010;120.2;438.15; 880.0
component=C10 paraffins;  0.056;142.3;433.15; 720.0
component=C10 cycloparaffins;  0.035;140.3;444.15; 800.0
component=C10 aromatics;  0.023;134.2;450.15; 860.0
component=C11 paraffins;  0.087;156.3;469.15; 740.0
component=C11 cycloparaffins;  0.033;154.3;469.15; 800.0
component=Dicycloparaffins;  0.031;152.3;474.15; 890.0
component=C11 aromatics;  0.036;148.2;478.15; 860.0
component=C12 paraffins;  0.108;170.3;489.15; 750.0
component=C12 cycloparaffins;  0.080;166.3;494.15; 880.0
component=C12 aromatics;  0.046;162.3;489.15; 860.0
component=C13 paraffins;  0.115;184.4;508.15; 760.0
component=C13 cycloparaffins;  0.085;182.4;498.15; 800.0
component=C13 aromatics;  0.049;176.3;507.15; 870.0
```

```
component=C14 paraffins;  0.059;198.4;527.15; 760.0
component=C14 cycloparaffins;  0.044;192.4;563.15; 940.0
component=C14 aromatics;  0.025;186.3;568.15;1030.0
component=C15 paraffins;  0.014;212.4;544.15; 770.0
component=C15 cycloparaffins;  0.010;206.4;573.15; 900.0
component=C15 aromatics;  0.006;200.4;578.15; 950.0
component=C16 hydrocarbons;  0.002;226.4;560.15; 770.0
component=Residual hydrocarbons;0.001;202.3;666.15;1270.0
```

Appendix C. The **getmet** *Utility*

C.1 Description

Some form of environmental data is required to run the integrated model. Although standard atmosphere data files can be used (see Appendix D), we demonstrated earlier (Section 4.6) the value of using current meteorological data near the site of the jettison event.

Current, raw (not decoded) upper air data can be obtained over the internet [1]. As of this writing (October 1994), Florida State University operates a gopher server for meteorological data, available on the internet at *metlab1.met.fsu.edu.* On Air Force installations, the local base weather station can provide this upper air data.

To facilitate formatting raw meteorological data for the model-ready environmental data file, we created the utility **getmet**.

A complete code listing is available in electronic format via anonymous ftp to

archive.afit.af.mil

in the directory

/pub/kpfeiffe/getmet.zip

Appendix D. The **makestd** *Utility*

To facilitate comparsion of our current work with previous results, we require a method to recreate standard atmosphere profiles based on a surface temperature, assumed to be sea-level temperature. The **makestd** utility is a small ANSI C code to generate this data based on a single input, the sea-level temperature in Celsius. This utility was used to produce the adjusted standard atmosphere data files used in the studies presented.

A complete code listing is available in electronic format via anonymous ftp to

archive.afit.af.mil

in the directory

/pub/kpfeiffe/makestd.zip

Bibliography

1. Ahlquist, Jon. "Free Software and Information via Computer Network," *Bulletin of the American Meteorological Society*, *74*(3):377–386 (March 1993).

2. Arfken, George. *Mathematical Methods for Physicists* (Third Edition). Orlando, Florida: Academic Press, 1985.

3. Atkins, P.W. *Physical Chemistry*. San Franciso: W.H. Freeman and Co., 1982.

4. Bilanin, Alan J., et al. "AGDISP: The Aircraft Spray Dispersion Model, Code Development and Experimental Validation," *Transactions of the American Society of Agricultural Engineers*, *32*(1):327–334 (January–February 1989).

5. Bird, R. Byron, et al. *Transport Phenomena*. New York: John Wiley and Sons, Inc., 1960.

6. Boas, Mary L. *Mathematical Methods in the Physical Sciences*. New York: John Wiley and Sons, 1983.

7. Burden, Richard L. and J. Douglas Faires. *Numerical Analysis* (Third Edition). Boston: Prindle, Weber, and Schmidt, 1985.

8. Clewell, Harvey J. *Evaporation and Groundfall of JP-4 Jet Fuel Jettisoned by USAF Aircraft*. Technical Report, Tyndall AFB, FL: Air Force Engineering and Services Center, September 1980. ESL-TR-80-56 (AD-A109307).

9. Clewell, Harvey J. *Fuel Jettisoning by U.S. Air Force Aircraft, Volume I: Summary and Analysis*. Technical Report, Tyndall AFB, FL: Air Force Engineering and Services Center, March 1980. ESL-TR-80-17 (AD-A089010).

10. Clewell, Harvey J. *Fuel Jettisoning by U.S. Air Force Aircraft, Volume II: Fuel Dump Listings*. Technical Report, Tyndall AFB, FL: Air Force Engineering and Services Center, March 1980. ESL-TR-80-17 (AD-A089076).

11. Clewell, Harvey J. *The Effect of Fuel Composition on Groundfall from Aircraft Fuel Jettisoning*. Technical Report, Tyndall AFB, FL: Air Force Engineering and Services Center, March 1981. ESL-TR-81-13 (AD-A110305).

12. Clewell, Harvey J. "Ground contamination by fuel jettisoned from aircraft in flight," *Journal of Aircraft*, *20*(4):382–384 (April 1983).

13. Cross, N.L. and R.G. Picknett. "Ground Contamination by Fuel Jettisoned from Aircraft," *Advisory Group for Aerospace Research and Development (AGARD) Conference Proceedings No. 125*, Chapter 12 (1973).

14. Dawbarn, R., et al. *A Study of Jettisoning of JP-4 Fuel Into the Atmosphere*. Technical Report, Arnold Air Force Station, TN: Arnold Engineering Development Center, November 1975. AEDC-TR-75-49 (AD-A017555).

15. Hanna, Steven R., et al. *Handbook on Atmospheric Diffusion*. Technical Information Center, US Department of Energy, 1982. DOE/TIC-11223.

16. Henderson-Sellers, Ann and Peter J. Robinson. *Contemporary Climatology*. Essex, England: Longman Scientific and Technical, 1986.

17. Hess, Seymour L. *Introduction to Theoretical Meteorology*. Malabar, Florida: Robert E. Krieger Publishing Co. Inc., 1959.

18. Holman, J.P. *Heat Transfer* (Fifth Edition). New York: McGraw-Hill, 1981.

19. Holton, James R. *Introduction to Dynamic Meteorology* (Second Edition). Orlando, Florida: Academic Press, 1979.

20. Lewellen, W.S. and R.I. Sykes. "Meteorological data needs for modeling air quality uncertainties," *Journal of Atmospheric and Oceanic Technology*, *6*:759–768 (October 1989).

21. Lowell, Herman H. *Dispersion of Jettisoned JP-4 Jet Fuel by Atmospheric Turbulence, Evaporation, and Varying Rates of Fall of Fuel Droplets*. Technical Report, Washington, DC: National Aeronautics and Space Administration, October 1959. NASA TN D-84.

22. Lowell, Herman H. *Free Fall and Evaporation of JP-4 Jet Fuel Droplets in a Quiet Atmosphere*. Technical Report, Washington, DC: National Aeronautics and Space Administration, September 1959. NASA TN D-33.

23. Lowell, Herman H. *Free Fall and Evaporation of JP-1 Jet Fuel Droplets in a Quiet Atmosphere*. Technical Report, Washington, DC: National Aeronautics and Space Administration, March 1960. NASA TN D-199.

24. Merrington, A.C. and E.G. Richardson. "The Break-up of Liquid Jets," *Proceedings of the Physical Society (London)*, *59*:1–13 (January 1947).

25. R.A. Wasson, Jr., et al. *Droplet Diameter and Size Distribution of JP-4 Fuel Injected into a Subsonic Airstream*. Technical Report, Arnold Air Force Station, TN: Arnold Engineering Development Center, April 1975. AEDC-TR-74-117 (AD-A007687).

26. Saucier, Walter J. *Principles of Meteorological Analysis*. New York: Dover Publications, Inc., 1983.

27. Seinfeld, John H. *Atmospheric Chemistry and Physics of Air Pollution*. New York: John Wiley and Sons, Inc., 1986.

28. Shames, Irving H. *Mechanics of Fluids*. New York: McGraw-Hill Book Company, 1962.

29. Sommerfeld, Arnold. *Partial Differential Equations in Physics*. New York: Academic Press, 1949.

30. Strikwerda, John C. *Finite Difference Schemes and Partial Differential Equations*. Pacific Grove, CA 93950: Wadsworth and Brooks, 1989.

31. Teske, Milton E., et al. "FSCBG: An aerial spray dispersion model for predicting the fate of released material behind aircraft," *Environmental Toxicology and Chemistry*, *12*:453–464 (1993).

32. United States Committee on Extension to the Standard Atmosphere. *U.S. Standard Atmosphere, 1976*. Washington: National Oceanic and Atmospheric Administration (NOAA), 1976.

33. Wark, Kenneth and Cecil F. Warner. *Air Pollution: Its Origin and Control*. Harper Collins Publishers, 1981.

34. Zannetti, Paolo. *Air Pollution Modeling: Theories, Computational Methods, and Available Software*. New York: Van Nostrand Reinhold, 1990.

Vita

Capt Pfeiffer was born in Biloxi, Mississippi on 11 November 1965. He attended the University of West Florida in Pensacola, Florida and graduated cum laude with a Bachelor of Science in Physics in 1988.

Capt Pfeiffer attended the Air Force Institute of Technology (AFIT) at the University of Oklahoma for the Basic Meteorology Program in 1989. In 1990 he was assigned to the 21 AF (MAC) Headquarters, McGuire AFB, New Jersey as Assistant Chief, Weather Support Unit. In 1992 Capt Pfeiffer was assigned to Military Airlift Command (MAC) Headquarters, Scott AFB, Illinois as Weather Systems Manager, Weather Support Unit. In 1993 he was selected to attend AFIT in residence at Wright Patterson Air Force Base, Dayton, Ohio for completion of a Master of Science in Computer Science.

Capt Pfeiffer is married to the former Ms Karen Whigham (Pensacola, Florida). Capt and Mrs Pfeiffer have a four-year-old son, Karl.

Permanent address: 5755 Ventura Lane
Pensacola, Florida 32526

REPORT DOCUMENTATION PAGE

Form Approved
OMB No. 0704-0188

Public reporting burden for this collection of information is estimated to average 1 hour per response, including the time for reviewing instructions, searching existing data sources, gathering and maintaining the data needed, and completing and reviewing the collection of information. Send comments regarding this burden estimate or any other aspect of this collection of information, including suggestions for reducing this burden, to Washington Headquarters Services, Directorate for Information Operations and Reports, 1215 Jefferson Davis Highway, Suite 1204, Arlington, VA 22202-4302, and to the Office of Management and Budget, Paperwork Reduction Project (0704-0188), Washington, DC 20503.

1. AGENCY USE ONLY (Leave blank)	2. REPORT DATE	3. REPORT TYPE AND DATES COVERED
	December 1994	Master's Thesis

4. TITLE AND SUBTITLE

A NUMERICAL MODEL TO PREDICT THE FATE OF JETTISONED AVIATION FUEL

5. FUNDING NUMBERS

6. AUTHOR(S)

Karl D. Pfeiffer, Capt, USAF

7. PERFORMING ORGANIZATION NAME(S) AND ADDRESS(ES)

Air Force Institute of Technology, WPAFB OH 45433-6583

8. PERFORMING ORGANIZATION REPORT NUMBER

AFIT/GCS/ENC/94D-01

9. SPONSORING/MONITORING AGENCY NAME(S) AND ADDRESS(ES)

AL/EQS
Tyndall AFB, FL 32403

10. SPONSORING/MONITORING AGENCY REPORT NUMBER

11. SUPPLEMENTARY NOTES

12a. DISTRIBUTION/AVAILABILITY STATEMENT

Distribution Unlimited

12b. DISTRIBUTION CODE

13. ABSTRACT *(Maximum 200 words)*

While airborne, military and civilian aircraft must occasionally jettison unburned aviation fuel into the atmosphere. This research investigates the fate of a jettisoned fuel (e.g. JP-4, JP-8, etc.) from initial release to final ground fall by numerically modeling the physical phenomena governing the fate of this fuel: evaporation, advection, and dispersion. Using previous work in evaporation and free fall of fuel droplets as a foundation, this thesis presents an integrated evaporation, advection and dispersion model designed to run under the resources of a typical personal computer. This integrated model is capable of using near real-time meteorological data (i.e. vertical profiles of temperature, pressure and wind) in all model calculations. Physical assumptions in the numerical model are presented, along with sample model calculations supporting these assumptions. Model calculations performed for two jettison scenarios show good agreement with previously published results.

14. SUBJECT TERMS

fuel jettison, ground contamination, dispersion model, mathematical model, aviation fuel, JP-4, JP-8

15. NUMBER OF PAGES

106

16. PRICE CODE

17. SECURITY CLASSIFICATION OF REPORT	18. SECURITY CLASSIFICATION OF THIS PAGE	19. SECURITY CLASSIFICATION OF ABSTRACT	20. LIMITATION OF ABSTRACT
UNCLASSIFIED	UNCLASSIFIED	UNCLASSIFIED	UL